

Semiclassical expectation values by adiabatic switching: Trapping and tunneling in the chaotic regime

B. Ramachandran*

Department of Chemistry and Institute for Theoretical Chemistry, University of Texas, Austin, Texas 78712

Kenneth G. Kay

Department of Chemistry, Bar-Ilan University, Ramat-Gan, Israel 52100

(Received 19 September 1989)

The adiabatic switching technique is adapted to the calculation of expectation values for chaotic systems. Semiclassical results obtained in this manner are compared to accurate quantum expectation values for the Hénon-Heiles system at high energy. Although good agreement is found for most states, the incidence of discrepancies grows as the energy increases. Almost all such discrepancies can be attributed to either quantum trapping effects for states with extreme values of quantum numbers or tunneling effects associated with the avoided crossings of energy curves as a function of a parameter in the Hamiltonian. As the energy is raised and the system becomes more chaotic, the increased strength of the avoided crossings leads to more frequent and stronger tunneling. The possible generality of this result and its implications for statistical quantum behavior are discussed.

I. INTRODUCTION

The relationship between classical and quantum mechanics in the domain where the classical motion is chaotic has been a subject of intense scrutiny for many years.¹ Some of the similarities and differences between chaotic classical systems and their quantum analogs are now becoming established.²⁻⁸ This work seeks to contribute to this emerging picture by comparing properties of the quantizing trajectories to the analogous quantum properties for a familiar two-dimensional system in the chaotic regime.

The problem of relating quantum and classical behavior has proved to be more challenging for classically chaotic systems than for regular systems. In the regular domain, well-defined constants of motion, i.e., the classical actions, exist and the Einstein-Brillouin-Keller (EBK) quantization rules connect the two forms of dynamics. In the chaotic regime, well-defined actions do not exist, and so these rules are not, strictly speaking, applicable. The problem of quantization in the chaotic regime has been addressed by many workers, and as a result, several methods have become available.⁹⁻²⁹ Among these, many recent applications have been based on a class of techniques generally known as adiabatic switching methods.²²⁻²⁹ These techniques rely on the assumption of adiabatic invariance of actions as a nonintegrable perturbation is "turned on" infinitesimally slowly. In the present work, we use the time-dependent version of the adiabatic switching method^{22-28,30} (hereafter referred to simply as adiabatic switching or AS) to generate quantizing trajectories in the chaotic regime.

The successes of semiclassical quantization methods in the chaotic regime are widely attributed to the existence of "vague tori,"¹⁴ which are regions of phase space

characterized by "approximate" actions and enclosed by temporary dynamical barriers. These dynamical barriers are generally "porous," at least in some places, so that, given sufficient time, some of the trajectories leak out of the bounded regions.³¹⁻³⁷ Thus the vague tori are short-lived entities in phase space. As time progresses, the dynamical barriers become increasingly ineffective, and the ensuring exponential divergence of trajectories erases all vestiges of the phase-space structures. Theories that quantitatively estimate the flux across such barriers have been developed recently,³¹⁻³² and have generated considerable interest in the chemical physics community.³⁵⁻³⁷

Dynamical barriers that temporarily confine a quantum wave packet to certain regions of phase space have also been observed in quantum systems.^{2,3,5-7} Some of the bounded quantum regions can be related to the vague tori of the analogous classical systems. However, the behavior of a quantum system initially confined to such bounded regions may be strikingly different from the analogous classical behavior: if tunneling is disregarded, a quantum wave packet may remain forever localized in a bounded region of phase space, unless the classical flux across the dynamical barriers is at least on the order of \hbar . This means that, even when nonlinearity is large enough to destroy classical barriers to an extent that large-scale classical chaos has emerged, a quantum system may behave as if the barriers were more or less intact. The resulting *quantum suppression* of classical chaos has profound implications for any trajectory-based approach that hopes to gain insight into the *quantum* behavior of a system. In the present work, we shall see that, in order to describe quantum states in the chaotic regime by classical means, it is crucial to mimic somehow the suppression of chaos.

The primary objective of this paper is to compare the

quantum and classical descriptions of states for a classically chaotic system. To accomplish this, we develop a version of the AS method that simulates the quantum suppression of chaos and apply it to calculate semiclassical analogs of quantum expectation values for a set of dynamical properties. Comparisons of these expectation values with the exact quantum results reveal the existence of important quantum effects that limit the applicability of classical mechanics to the quantum analogs of chaotic systems. These effects therefore, have important implications for the ability of quantum systems to exhibit statistical behavior (i.e., ergodicity).

The remainder of this paper is based on the following plan. In Sec. II we discuss our approach to the calculation of semiclassical expectation values in the chaotic regime, in Sec. III, we compare the resulting semiclassical quantities to the exact quantum expectation values and discuss the significance of the results, and finally, in Sec. IV, we present a summary of our work.

II. SEMICLASSICAL EXPECTATION VALUES IN THE CHAOTIC REGIME

A. Semiclassical analogs of expectation values

According to the Heisenberg correspondence principle,³⁸⁻⁴⁰ the classical analog $\langle A \rangle_m$ of the quantum expectation value $\langle A \rangle_m^q \equiv \langle \mathbf{m} | A | \mathbf{m} \rangle$ is given by

$$\langle A \rangle_m = \frac{\int d\mathbf{p} \int d\mathbf{q} \delta(\mathbf{J}(\mathbf{p}, \mathbf{q}) - \mathbf{J}_m) A(\mathbf{p}, \mathbf{q})}{\int d\mathbf{p} \int d\mathbf{q} \delta(\mathbf{J}(\mathbf{p}, \mathbf{q}) - \mathbf{J}_m)}, \quad (1)$$

where \mathbf{J}_m is the vector containing the quantized values of the actions corresponding to quantum numbers \mathbf{m} , $\mathbf{J}(\mathbf{p}, \mathbf{q})$ is the vector containing the N action variables as functions of canonical coordinates \mathbf{q} and momenta \mathbf{p} , and $A(\mathbf{p}, \mathbf{q})$ is the classical function corresponding to the operator \hat{A} . The semiclassical expectation value $\langle A \rangle_m$ is thus a phase-space average of the property $A(\mathbf{p}, \mathbf{q})$ over a torus characterized by the quantizing actions \mathbf{J}_m .

We are interested in identifying the semiclassical analogs $\langle A \rangle_m$ in the chaotic regime of classical dynamics where well-defined actions do not exist. Strictly speaking, this would mean that Eq. (1) cannot be applied. However, *vague* tori do exist in the chaotic regime so that a set of actions is approximately conserved for a finite period of time. Thus we may attempt to adapt Eq. (1) to this case in the hope that there exist vague tori in the chaotic regime that are characterized by approximate actions that satisfy quantization conditions. To do this, we replace the δ function in Eq. (1) with a density function $\rho(\mathbf{J} - \tilde{\mathbf{J}}_m)$ which is identically equal to zero everywhere in phase space except on a vague torus characterized by the approximate actions $\tilde{\mathbf{J}}_m$. Thus, in the chaotic regime, we identify the semiclassical expectation value of property A over a state $|\mathbf{m}\rangle$ as

$$\langle A \rangle_m = \frac{\int d\mathbf{p} \int d\mathbf{q} \rho(\mathbf{J}(\mathbf{p}, \mathbf{q}) - \tilde{\mathbf{J}}_m) A(\mathbf{p}, \mathbf{q})}{\int d\mathbf{p} \int d\mathbf{q} \rho(\mathbf{J}(\mathbf{p}, \mathbf{q}) - \tilde{\mathbf{J}}_m)}. \quad (2)$$

In the present work, we generate well-defined, local-

ized, quantizing vague tori in the chaotic regime and compute $\langle A \rangle_m$ as averages of $A(\mathbf{p}, \mathbf{q})$ over this region. This procedure eliminates the need for an explicit expression for $\rho(\mathbf{J}(\mathbf{p}, \mathbf{q}) - \tilde{\mathbf{J}}_m)$. The restriction of the classical density to quantizing vague tori is intended to mimic the quantum suppression of chaos, which confines the quantum density associated with energy eigenstates to specific regions of phase space even when the classical density ultimately spreads over much of the energy surface. The generation of quantizing vague tori that are localized in specific portions of phase space therefore forms an important part of the present investigation. We discuss how this is accomplished in Sec. II B.

B. Generation of quantizing tori

We use the method of adiabatic switching to generate quantizing trajectories and vague tori for the system we wish to study. To motivate the discussion below and establish our terminology, we now briefly review the AS method.²²⁻³⁰

Consider a system described by a Hamiltonian $H(\mathbf{p}, \mathbf{q})$, which can be written as

$$H(\mathbf{p}, \mathbf{q}) = H_0(\mathbf{p}, \mathbf{q}) + H'(\mathbf{p}, \mathbf{q}),$$

where H_0 is rigorously integrable and H' is a nonseparable perturbation that renders H nonintegrable. By definition then, the dynamics of H_0 is regular and all trajectories generated by this Hamiltonian are confined to well-defined tori. Thus EBK quantization rules can be applied to H_0 to obtain a set of quantizing tori, characterized by actions \mathbf{J} . The adiabatic switching method assumes that if the perturbation is "turned on" infinitely slowly, the set of zeroth-order actions \mathbf{J} remains invariant, while the energies of the trajectories change from the quantized energies of the integrable system to those of the fully coupled system. The basis for this expectation is the classical adiabatic theorem. Although the theorem can be rigorously proved only in the one-dimensional case, a comparison of the results obtained from adiabatic switching with exact quantum results²²⁻²⁹ shows that the assumption is often satisfied to a high level of accuracy by multidimensional systems. In practical implementations of the method, the perturbation is, of course, turned on within a finite interval T , with the aid of a switching function $s(t)$, as follows:

$$H(\mathbf{p}, \mathbf{q}, t) = H(t) = H_0 + s(t)H' \quad \text{for } 0 \leq t \leq T, \\ s(0) = 0, \quad s(T) = 1.$$

Existing studies of the method shows that a careful choice of H_0 , $s(t)$, and T leads to reliably accurate semiclassical energies even in the chaotic regime.²³⁻²⁸

The success of the adiabatic switching method in quantizing the chaotic part of phase space has been attributed to the existence of tori for a significant part of the switching process.²³ Even when tori break down as the coupling H' becomes stronger, dynamical barriers or "bottlenecks" tend to confine trajectories to regions in the close vicinity of the destroyed tori, thus approximately conserving the actions \mathbf{J} . The degree of conservation

of these actions in the adiabatic switching calculation of a particular energy level can be estimated by examining ΔE_{rms} , the root-mean-square deviation in the final energy for an ensemble of initial points distributed over the torus of the zeroth-order system. The less accurate conservation of the J for chaotic systems is reflected in the larger values ΔE_{rms} for the computed energies in the chaotic regime. However, as long as the ΔE_{rms} are smaller than the spacings between adjacent quantized energy levels, the method succeeds in resolving these levels in chaotic systems. In this paper we use the AS technique to compute semiclassical expectation values of certain dynamical properties in a chaotic system.

The system that we choose for the present investigations is the Hénon-Heiles system.⁴¹ The Hamiltonian for this system is given by

$$H = \frac{1}{2}(p_x^2 + x^2 + p_y^2 + y^2) + \lambda x(y^2 - x^2/3),$$

where the value of the perturbation parameter λ is set at 0.08. This system possesses 380 (quasi)bound levels below the dissociation energy $1/6\lambda^2 = 26.04$. The dynamical properties A for which we calculate expectation values $\langle A \rangle$ in this system are

$$\begin{aligned} H_0 &= \frac{1}{2}(p_x^2 + x^2 + p_y^2 + y^2), \\ L &= xp_y - yp_x, \\ L^2 &= (xp_y - yp_x)^2, \\ D &= \frac{1}{2}(p_x^2 + x^2 - p_y^2 - y^2), \\ P &= p_x p_y + xy. \end{aligned} \quad (3)$$

The Hénon-Heiles potential belongs to the C_{3v} point group. In the regular regime of this system (low energy), trajectories are confined mainly to two types of tori:⁴² the librating type and the precessing type. The librating tori occur in sets of three, bear trajectories of low angular momentum, and are confined to regions close to the three C_2 symmetry axes of the potential. The precessing tori, on the other hand, bear trajectories of higher angular momentum, and occur in pairs corresponding to clockwise and counterclockwise motion around the potential well. The adiabatic switching method requires two different H_0 's to generate the librating and precessing tori. To form the librating tori, we choose^{23,30}

$$H_0 = \frac{1}{2}(p_x^2 + 0.81x^2 + p_y^2 + y^2), \quad (4)$$

so that $H' = \lambda x(y^2 - x^2/3) + 0.19x^2$, and quantize the zeroth-order actions

$$\begin{aligned} J_x &= (2\pi)^{-1} \oint p_x dx, \\ J_y &= (2\pi)^{-1} \oint p_y dy \end{aligned} \quad (5)$$

by requiring that

$$\begin{aligned} J_x &= (n_x + \frac{1}{2}) \quad (n_x = 0, 1, 2, \dots), \\ J_y &= (n_y + \frac{1}{2}) \quad (n_y = 0, 1, 2, \dots). \end{aligned} \quad (6)$$

Two other topological equivalents of the librating torus generated from these initial conditions are obtained by

rotating the switched torus through 120° and 240° , respectively.

To form the precessing tori we choose^{23,30}

$$H_0 = \frac{1}{2}(p_x^2 + x^2 + p_y^2 + y^2), \quad (7)$$

and quantize the zeroth-order actions

$$\begin{aligned} J_n &= \pi^{-1} \oint p_r dr + (2\pi)^{-1} \oint p_\theta d\theta, \\ J_l &= (2\pi)^{-1} \oint p_\theta d\theta, \end{aligned} \quad (8)$$

by requiring that

$$\begin{aligned} J_n &= n + 1 \quad (n = 0, 1, 2, \dots), \\ J_l &= l \quad (l = \mp n, \mp(n-2), \dots). \end{aligned} \quad (9)$$

Here, r and θ are conventional polar coordinates. The direction of the motion of trajectories on the final precessing torus generated by AS from these initial conditions is determined by the sign of p_θ . Thus, if the torus generated by AS bears trajectories that travel in the clockwise sense, the torus bearing trajectories that precess in the counterclockwise sense can be generated by simply reversing the sign of J_l .

To calculate the classical expectation value $\langle A \rangle_m$, the average in Eq. (2) is evaluated by the Monte Carlo method as

$$\langle A \rangle_m \cong N^{-1} \sum_{i=1}^N A(\mathbf{p}_i, \mathbf{q}_i), \quad (10)$$

where the summation runs over N points randomly distributed over the vague torus. These points are generated by applying the AS method to an ensemble of points on the zeroth-order torus with action variables as described above and angle variables randomly and uniformly distributed on the interval $(0, 2\pi]$.³⁰ That this procedure indeed results in the formation of a uniformly weighted, random distribution of points on the evolved vague torus follows from the work of Skodje and Borondo.⁴³

C. Quantum calculation and assignment of quantum states

To form quantum expectation values, the energy eigenfunctions and eigenvalues for the Hénon-Heiles system are calculated by diagonalization of the Hamiltonian in a basis of isotropic harmonic oscillators f_{nl} which includes all functions with $n \leq 75$. This basis is substantially larger than the one used in the previous investigation of this system^{44,6} and yields energy eigenvalues that are converged to at least five significant figures for all levels investigated in this paper.

The energy eigenstates of the system are classified as belonging to the A_1 , A_2 , or E irreducible representations of the C_{3v} point group. The vague tori obtained by the AS procedure, however, are labeled by either $[n_x, n_y]$ quantum numbers (in the case of librating tori) or (n, l) quantum numbers (in the case of precessing tori). To compare the results of the quantum and AS calculations, it is necessary to identify quantum states with AS tori, i.e., to assign $[n_x, n_y]$ or (n, l) quantum numbers to the quantum states. We accomplish this in an *ad hoc*

manner by associating each quantum state with the AS torus having the most similar values for the energy and the $\langle A \rangle$. The resulting quantum number assignments are somewhat different than those previously reported⁴⁴ due to the use of a larger basis in the current calculations. These assignments are presented in Sec. III.

The assignment of zeroth-order quantum numbers to the states of our system is problematic⁴⁴ for energy levels that undergo avoided crossings as functions of λ near $\lambda=0.08$. This complication is discussed in Sec. III. Another complication arises from dynamic tunneling between tori located in symmetrically related regions of phase space.^{13,44,45} It is well-known that such tunneling causes the energy eigenstates to be delocalized among the symmetry-related tori and at least partly lifts the degeneracy of their energy levels. To form quantum states that are localized in regions occupied by the tori, it is thus necessary to form superpositions^{44,45} of the energy eigenstates involved in the tunneling process. The quantum expectation values computed over such superposition states are obviously the most appropriate quantities to be compared with the semiclassical expectation values computed over the quantizing tori. It is clear that these arguments can be extended to the chaotic regime by relating quantum superposition states to quantizing *vague* tori. We now describe the theoretical considerations which determine these superpositions.

The following characteristics of the Hénon-Heiles system are well known. Certain pairs of A_1 and A_2 states are separated by relatively small energy differences. Such pairs of states generally have intermediate to high values of the zeroth-order quantum number l and are assigned the same n and l quantum numbers. Previous studies⁴² have shown that these states are analogous to the precessing (*vague*) tori. The semiclassical degeneracy of the two precessing tori bearing trajectories that travel in the clockwise and counterclockwise senses is lifted in the quantum mechanical system by dynamical tunneling between the two tori.¹³ It seems reasonable, then, for the present purposes, to combine such A_1 - A_2 pairs to form superpositions that correspond to the semiclassical tori. The doubly degenerate E states can be represented as complex states or as real states formed by superposing the complex states. Examination of the expectation values suggests that some of the doubly degenerate complex E states which are assigned intermediate to high values of the $|l|$ quantum number also correspond to precessing tori. The states corresponding to the precessing tori in the semiclassical limit are therefore⁴⁴

$$\begin{aligned} &(|a_1\rangle + i|a_2\rangle)/2^{1/2}, \\ &(|a_1\rangle - i|a_2\rangle)/2^{1/2}, \\ &|e\rangle, |e^*\rangle. \end{aligned}$$

Similarly, certain states of A symmetry (A_1 or A_2) occur very close in energy to states of E symmetry. In these cases, the expectation values suggest that the A state as well as the degenerate E states be assigned low values of the angular momentum quantum number l . In an earlier investigation of the AS method, Grozdanov, Saini, and

Taylor²⁶ observed that the semiclassical analogs of such sets of states seem to be the three librating tori. The energy splitting between the states of A and E symmetry, then, arises from dynamical tunneling among the three symmetrically equivalent tori. It therefore seems reasonable to combine these sets of three states to form three superposition states that are topologically similar to the classical librators. The appropriate superpositions are of the type⁴⁴

$$\begin{aligned} &(\frac{1}{3})^{1/2}|a_1\rangle + c(\frac{2}{3})^{1/2}|e_x\rangle, \\ &(\frac{1}{3})^{1/2}|a_1\rangle - c(\frac{1}{6})^{1/2}|e_x\rangle + c(\frac{1}{2})^{1/2}|e_y\rangle, \\ &(\frac{1}{3})^{1/2}|a_1\rangle - c(\frac{1}{6})^{1/2}|e_x\rangle - c(\frac{1}{2})^{1/2}|e_y\rangle, \end{aligned}$$

or

$$\begin{aligned} &(\frac{1}{3})^{1/2}|a_2\rangle + c(\frac{2}{3})^{1/2}|e_y\rangle, \\ &(\frac{1}{3})^{1/2}|a_2\rangle - c(\frac{1}{6})^{1/2}|e_y\rangle + c(\frac{1}{2})^{1/2}|e_x\rangle, \\ &(\frac{1}{3})^{1/2}|a_2\rangle - c(\frac{1}{6})^{1/2}|e_y\rangle - c(\frac{1}{2})^{1/2}|e_x\rangle, \end{aligned}$$

where $c = \pm 1$, $|e_x\rangle = [|e\rangle + |e^*\rangle] / 2^{1/2}$, and $|e_y\rangle = [|e\rangle - |e^*\rangle] / (2^{1/2}i)$.

It is useful, for our discussion below, to describe the relationship between the $(n, |l|)$ assignments for states with low values of $|l|$ and the more appropriate $[n_x, n_y]$ quantum numbers that label the librating tori obtained from AS. For states with an even value of n , the l quantum number assumes the values $0, \pm 2, \pm 4, \dots, \pm n$, while for odd values of n , the allowed l values are $\pm 1, \pm 3, \dots, \pm n$. States of A symmetry are labeled by values of $|l|$ that are 0 or multiples of 3. The $[n_x, n_y]$ quantum numbers satisfy the condition $n_x + n_y = n$, and the progression of the quantum numbers is given by $[n_x, n_y] = [n, 0], [n-1, 1], [n-2, 2], \dots$. Indicating the states in a superposition by enclosing them in braces, the relations between the assignments $(n, |l|)$ (denoted by parentheses) and the $[n_x, n_y]$ (denoted by square brackets) are given by

$$\begin{aligned} \{(n, 0), (n, \pm 2)\} &\equiv [n, 0], \\ \{(n, \pm 4), (n, \pm 6)\} &\equiv [n-1, 1], \\ \{(n, \pm 6), (n, \pm 8)\} &\equiv [n-2, 2], \end{aligned}$$

for even n , and

$$\begin{aligned} \{(n, \pm 1), (n, \pm 3)\} &\equiv [n, 0], \\ \{(n, \pm 3), (n, \pm 5)\} &\equiv [n-1, 1], \\ \{(n, \pm 7), (n, \pm 9)\} &\equiv [n-2, 2], \end{aligned}$$

for odd n . Note that the states labeled by $|l|$ that are multiples of 3 correspond to pairs of A_1 and A_2 states. Since only one member of this pair is involved in a certain librating type superposition, the other can be used in *another* superposition. Thus each of the states labeled $(n, \pm 3)$ and $(n, \pm 6)$ appears in two superpositions. We do not form librating-type superpositions with $n_y > 2$ since trajectories corresponding to the higher values of n_y are no longer confined to the librating regions of phase space in our system. Generation of such tori by AS using the

initial conditions of Eqs. (5) and (6) would therefore involve a change in the topology of the evolving torus at some state during the switching. This would correspond to a crossing of the precessor-librator separatrix and would result in a breakdown of the adiabatic assumption.²³ The quantizing tori with $n_y > 2$ are, therefore, generated by the precessing-type initial conditions of Eqs. (8) and (9), and are labeled by (n, l) quantum numbers.

D. The switching process

We now turn to the practical aspects of implementing the AS method. The switching function $s(t)$ is chosen to have the form

$$s(t) = t/T - \sin(2\pi t/T)/2\pi. \quad (11)$$

This switching function has been used in several previous studies.^{23,24,28,30} It has been shown to yield semiclassical energies of good accuracy and small values of ΔE_{rms} , provided that the switching time T is chosen appropriately.

The choice of T must take into account two conflicting requirements. First, T must not be so long that the evolving trajectories are significantly influenced by chaos, causing the large-scale destruction of tori. Under such circumstances (i) actions are obviously not conserved so that the theoretical basis of the AS method breaks down, and (ii) the classical calculations fail to mimic the quantum suppression of chaos which should confine state density to phase-space regions resembling intact tori. On the other hand, T must not be chosen so small that nonadiabaticity becomes severe, causing poor conservation of the actions, and large values of ΔE_{rms} . Under these circumstances, the final trajectories will not lie on accurate

tori or vague tori and the semiclassical calculations will be subject to large errors.

To illustrate these points, we apply the AS method to the zeroth-order tori labeled by [22,2] and (24,12). These tori evolve into vague tori that are typical of those in the chaotic regime of the fully coupled system. The value of T we use for the switching process is 300, which is smaller than the value of 400 used by Skodje, Borondo, and Reinhardt²³ and others^{26,27} in applications of the AS method to the Hénon-Heiles Hamiltonian with $\lambda=0.1118$ but large enough to ensure that the ΔE_{rms} values are reasonably small. The final average energies of the trajectories and the ensemble averages of the six properties for the two states are presented in the first column of Table I, while the exact quantum results, computed over superposition states, are presented in the second column. It is immediately apparent from Table I that the semiclassical ensemble averages are in very poor agreement with the quantum expectation values. The semiclassical energy of the state [22,2] is also considered to be in error, since the exact quantum energy does not fall within $\pm\Delta E_{\text{rms}}$ of the AS energy.

Figure 1, which shows the Poincaré surfaces compiled at the end of the switching, helps explain these results. Figure 1(a) shows the final Poincaré surface of state [22,2] using the $s(t)$ of Eq. (11). It is clear from this figure that, although some vestiges of a librating vague torus are identifiable, many trajectories have already wandered away from the phase-space region associated with it. The poor conservation of actions due to this disintegration of the vague torus is reflected in the inaccuracies in the semiclassical energies and expectation values.

Figure 1(b) shows the Poincaré surface of state (24,12). We see that the precessing vague torus corresponding to

TABLE I. Comparison of the exact quantum expectation values $\langle A \rangle_q$ to the semiclassically expectation values $\langle A \rangle$ generated by different switching functions.

Property	$s(t)^a$	Quantum ^b	$s(u)^c$
State [22,2]			
E	23.420±0.034 ^d	23.464	23.474±0.034 ^d
H_0	27.35±0.36	27.01	26.95±0.30
L	0.95±0.70	0.0	0.22±0.77
L^2	159±9	178	191±9
D	-2.23±0.95	-9.02	-9.26±0.94
P	-1.63±1.02	-15.62	-15.66±0.96
State (24,12)			
E	23.700±0.038 ^d	23.724	23.718±0.039 ^d
H_0	27.58±0.38	27.04	26.97±0.31
L	2.77±0.73	7.13	7.67±0.68
L^2	177±9	202	208±9
D	0.67±1.03	0.0	0.97±0.95
P	-1.15±0.95	0.0	0.82±0.91

^aSemiclassical expectation values obtained by using the switching function $s(t)$.

^bQuantum expectation values.

^cSemiclassical expectation values obtained by using the switching function $s(u)$.

^dThe errors reported in these cases are ΔE_{rms} values. The errors for the other properties are Monte Carlo errors μ_A .

this state is also in the process of disintegrating, although it is somewhat better preserved than that of Fig. 1(a). Not too surprisingly, the exact quantum energy of this state falls within the standard deviation ΔE_{rms} of the semiclassical

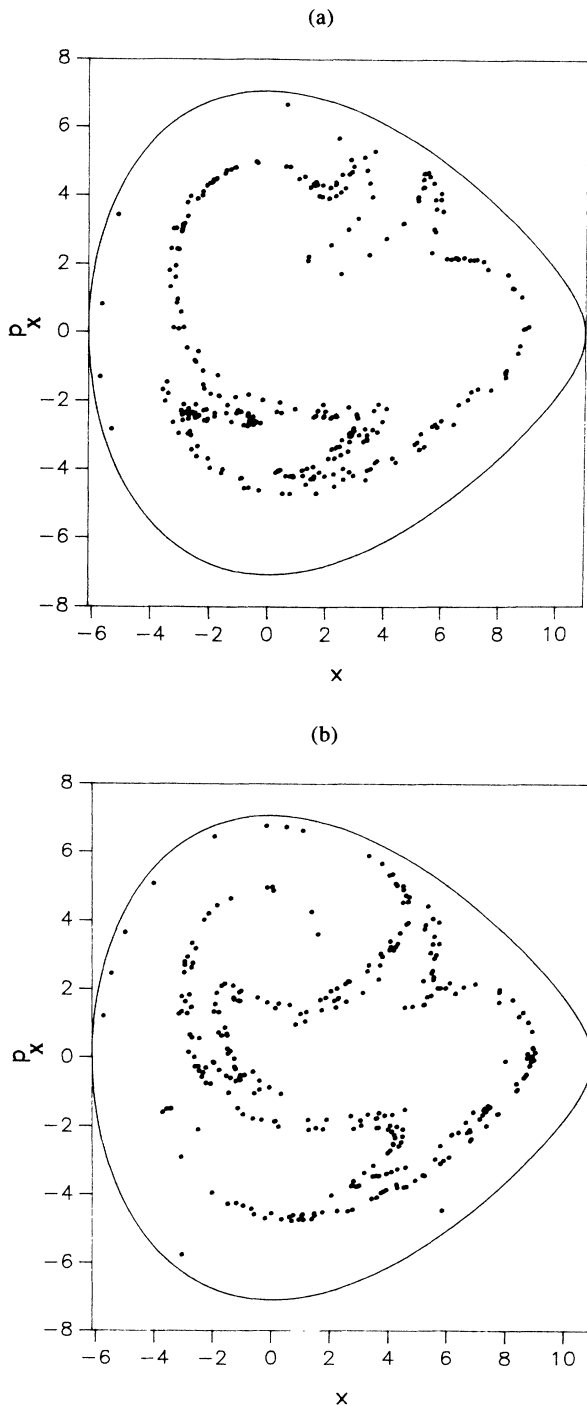


FIG. 1. Poincaré surfaces of section generated at the end of adiabatic switching using the switching function $s(t)$ for (a) state [22,2], and (b) state (24,12). Only the last intersection before completion of switching is plotted for each of 320 trajectories.

energy. However, the ensemble averages of properties A for this state, especially those of L and L^2 , do not agree well with the exact quantum results. This suggests that the semiclassical expectation values $\langle A \rangle$ are far more sensitive to the influence of chaos on the switched trajectories than are the semiclassical energies.

From our discussions above concerning the choice of T , it would seem that a smaller T might reduce the influence of chaos on the trajectories. We have, indeed, found this to be the case. However, the values of T required to bring the ensemble averages even into approximate agreement with the exact quantum expectation values for chaotic states are so small that the ΔE assume unacceptably large values.

There is, however, an alternative to the above method for reducing the influence of chaos, which has the advantage of maintaining acceptably small values for the ΔE_{rms} . This technique is suggested by two observations: (i) the symptoms of chaos on an evolving torus become detectable only towards the end of the switching process, when the perturbation due to H' becomes sufficiently large, i.e., when the switching function $s(t)$ becomes larger than a certain value, which we denote by s_c ; and (ii) for regular states and sufficiently long switching times T , the nonadiabaticity in the switching process (as measured by ΔE_{rms}) is largely a function of the rate of the switching process and the smoothness of the switching function. This implies that we should be able to minimize the effects of chaos on the switched tori while maintaining a high level of adiabaticity by using a smooth "accelerated" switching function that slowly increases with time t from $s(0)=0$ to the chaotic threshold s_c , and then more rapidly traverses the range from s_c to 1, at which point the switching ends. Obviously, such a switching function can be defined in many ways. We choose the function to be $s(u(t))$, where s is the function defined in Eq. (11) and

$$u(t) = t[1 + \alpha f(t - \tau)], \quad (12)$$

where

$$f(x) = 1/[1 + \exp(-\beta x)]. \quad (13)$$

The parameters α , β , and τ in Eqs. (12) and (13) merit some discussion. The "acceleration" in the switching process begins in the neighborhood of $t = \tau$, so that $s(u(\tau))$ can be identified with s_c . The magnitude of the acceleration [i.e., $|s(u) - s(t)|$ for $t > \tau$] is determined by the parameter α ($u = t$ if $\alpha = 0$) and the "suddenness" of the acceleration is determined by the parameter β . Adiabatic switching using $s(u)$ ends when $s(u)$ reaches the value of 1, which occurs at some time $t < T$. Numerical values for the parameters α , β , and τ are chosen to yield trajectories that are relatively uninfluenced by chaos during the switching process and that yield AS energies with small ΔE_{rms} . By trial and error, we have found that these conditions are satisfied for the system investigated here by $\beta \leq 0.15$, $0.75T \leq \tau \leq 0.85T$, and a wide range of values of α (see below).

As an illustration of the use of $s(u)$ in adiabatic switching, we compute the quantized energies and the ensemble

averages of the properties in Eq. (6) for the same two states examined above. The results of adiabatic switching for these states using $s(u)$ instead of $s(t)$ (with $\alpha=10$, $\beta=0.10$, $\tau=245$, and $T=300$) are presented in the third column of Table I. It is immediately clear from a com-

parison of the columns in this table that the semiclassical energy of the state [22,2] is now in much better agreement with the exact quantum energy. The improvement in the agreement between the semiclassical $\langle A \rangle$ and the quantum $\langle A \rangle_q$ for this state and for the state (24,12) is also significant.

Poincaré surfaces for states [22,2] and (24,12) obtained at the end of the switching process using $s(u)$, are presented in Figs. 2(a) and 2(b), respectively. It is clear from a comparison of Fig. 2(a) to Fig. 1(a) and Fig. 2(b) to Fig. 1(b) that the vague tori are much better preserved when $s(u)$ is used instead of $s(t)$ for the switching. The differences between Figs. 1 and 2 translate into the large differences between the $\langle A \rangle$ listed in columns 1 and 3 of Table I. This confirms our earlier observation that the properties $\langle A \rangle$ are highly sensitive to the influence of chaos on the vague tori.

We now examine the sensitivity of the AS results to the "acceleration" parameter α in the switching function. Setting $\beta=0.10$, $\tau=245$, and $T=300$, we compute the $\langle A \rangle$ for a set of α values in the range $0 \leq \alpha \leq 20$ for states [22,2] and (24,12). Recall that the case $\alpha=0$ is equivalent to using $s(t)$ for the switching. The results for these two states are summarized in Fig. 3. The values of

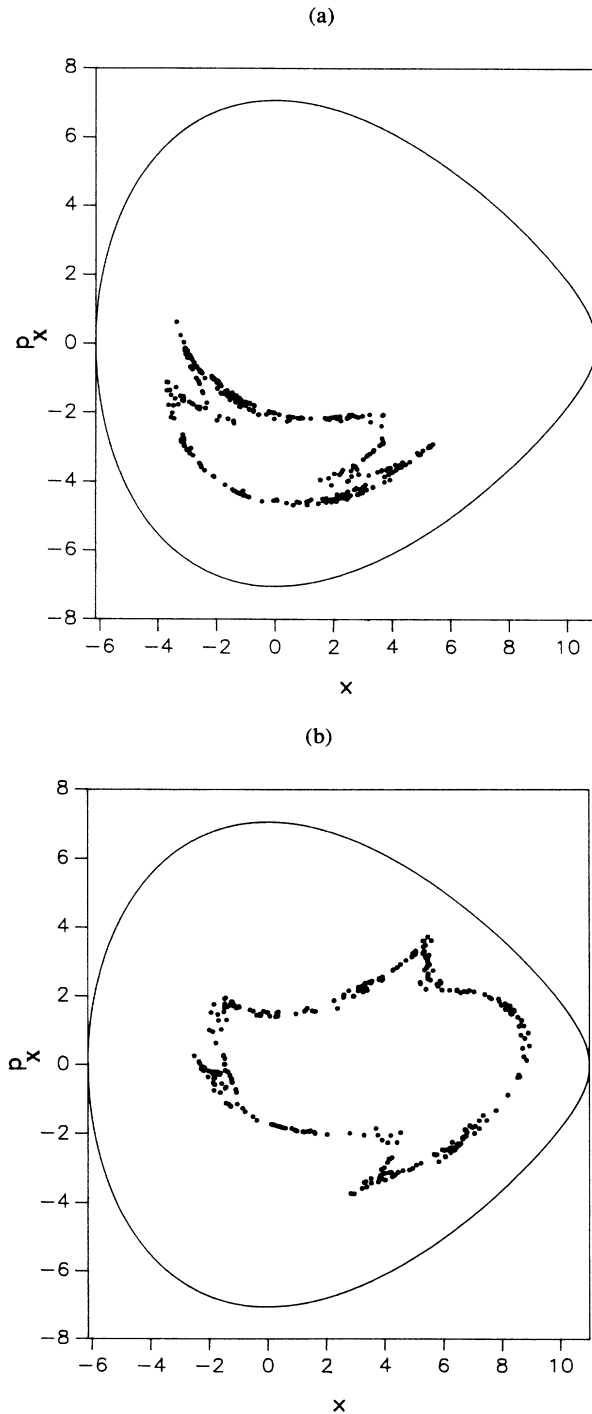


FIG. 2. Poincaré surfaces of section generated at the end of adiabatic switching using the switching function $s(u)$, for (a) state [22,2] and (b) state (24,12). Only the last intersection before completion of switching is plotted for each of 320 trajectories.

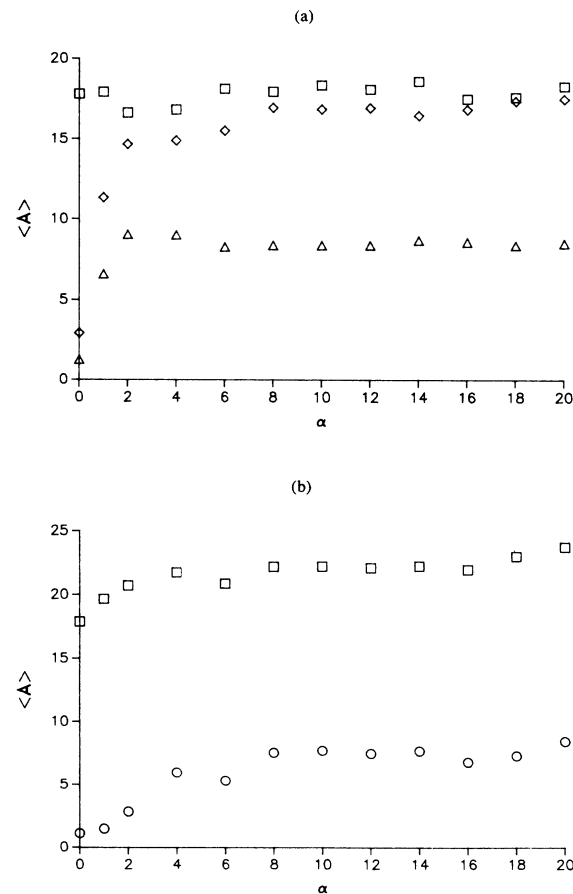


FIG. 3. The semiclassical expectation values as a function of the switching parameter α for (a) state [22,2] and (b) state (24,12). \circ , $\langle L \rangle$; \square , $\langle L^2 \rangle$; \triangle , $\langle D \rangle$; \diamond , $\langle P \rangle$. $\langle L^2 \rangle$ has been multiplied by a factor of 0.1 for clarity of presentation.

$\langle H_0 \rangle$ are largely insensitive to the parameters in $s(u)$, and hence the results for this property are not presented in this figure. The results for those $\langle A \rangle$ that are very small are also not reported in Fig. 3. These include $\langle L \rangle$ for [22,2] and $\langle D \rangle$ and $\langle P \rangle$ for (24,12).

Figure 3 shows that, as α is raised from 0 to about 6 or 8, the $\langle A \rangle$ vary over a fairly broad range in a seemingly irregular manner. However, for larger values of α , the $\langle A \rangle$ remain fairly constant. To understand these results, we recall that α determines the rate at which the chaotic range between s_c and 1 is traversed. When α is small, this range is traversed rather slowly, allowing considerable opportunity for the trajectories to be influenced by chaos. However, when α is large, this range is traversed rapidly enough that the trajectories cannot wander far from well-preserved vague tori. Since these vague tori occupy definite regions of the phase space, the resulting properties $\langle A \rangle$ have reasonably well-defined values and are relatively insensitive to further variations in α . Presumably, if the value of α were increased indefinitely, a point would be reached where the switching would be completed so quickly that the nonadiabaticity would become unacceptably high.

To generate semiclassical expectation values $\langle A \rangle$ for comparison with the exact quantum results, we apply the accelerated AS procedure to an ensemble of 320 trajectories for each state. We choose the parameters in the switching function to be $\beta=0.10$, $\tau=245$, and $T=300$ and repeat these calculations with three values of α : 8.0, 10.0, and 12.0. We compute the $\langle A \rangle$ over the ensemble of trajectories for each α and report the average of these three results and the standard deviation σ_A for comparison with the exact quantum expectation values. This comparison is the topic of Sec. III.

III. COMPARISON OF QUANTUM AND SEMICLASSICAL EXPECTATION VALUES

In this section, we examine and discuss the results of our calculations of semiclassical expectation values for states with n in the range 20–25. These states encompass a range of energy in which the dynamics of the classical Hénon-Heiles system varies from partly chaotic ($E=20$, where about half of the energy surface is occupied by regular trajectories) to mostly chaotic (near the dissociation energy at $E=26.04$, where only a small portion of the energy surface is occupied by regular trajectories).⁴⁶ To present our results in a systematic manner, we divide our discussion into four sections. In Sec. III A we examine the general trends in the $\langle A \rangle$ and the $\langle A \rangle_q$ as the (n, l) quantum numbers vary. In Sec. III B we examine discrepancies observed between the semiclassical and quantum results, and relate them to purely quantal phenomena such as quantum trapping and tunneling associated with avoided crossings. In Sec. III C we examine evidence that the tunneling observed here is a widespread phenomenon for chaotic systems. Finally, in Sec. III D we describe the possible implications of these results for the ability of quantum systems to display statistical behavior.

A. Semiclassical and quantum expectation values

Previous studies^{6,7,13,14,23,26,41,42,44,46} of the Hénon-Heiles system have generated a wealth of information regarding its dynamics. It is thus possible to anticipate the trends in the semiclassical expectation values $\langle A \rangle$ as functions of the quantum numbers. For states with very small values of $|l|$, the quantizing vague tori, labeled by $[n_x, n_y]$ quantum numbers, bear trajectories that are confined by barriers to regions close to the three C_2 axes of the Hénon-Heiles potential. The almost complete absence of any precessing character for these states is expected to be reflected in relatively small values of $\langle L^2 \rangle$, and corresponding large values of $\langle D \rangle$ and $\langle P \rangle$. As the value of n_y (or $|l|$) increases, the amplitude of the motion normal to the C_2 axes increases. This means that the values of $\langle L^2 \rangle$ increase, while those of $\langle D \rangle$ and $\langle P \rangle$ decrease. As $|l|$ increases further, more trajectories are able to surmount to barriers and precess, and the resulting vague tori are labeled by (n, l) quantum numbers. For such vague tori, $\langle L \rangle$ and $\langle L^2 \rangle$ should increase more or less monotonically as $|l|$ increases. Of course, in the absence of purely quantal phenomena, similar behavior is expected for the $\langle A \rangle_q$ as well. The quantum expectation values, however, can be shown to obey certain additional relationships. From the symmetry of the quantum superposition states, it can be proved that $\langle L \rangle_q \equiv 0$ and $\langle P \rangle_q = \sqrt{3} \langle D \rangle_q$ for the librating-type superpositions, while $\langle D \rangle_q = \langle P \rangle_q = 0$ for the precessing-type superpositions. If the classical-quantal correspondence is good, the classical $\langle A \rangle$ should satisfy similar relationships. The extent to which these relationships are indeed found to be satisfied provides an additional check for the success of the AS procedure.

We now summarize our results in the form of Figs. 4(a)–4(f), where the classical and quantum versions of $\langle L \rangle$, $\langle L^2 \rangle$, $\langle D \rangle$, and $\langle P \rangle$ are plotted for each n , as functions of $|l|$. The results for those states that have been quantized from zeroth-order tori $[n_x, n_y]$ are plotted at the mean value of $|l|$ for the superposition. For example, the state [22,0] corresponds to a superposition of the states labeled by (22,0) and (22,2). We thus plot the results for this state at $|l|=1$ in the appropriate figure. This convention is maintained in all six subfigures. We do not present the results for the $\langle H_0 \rangle$ in these figures because the differences between $\langle H_0 \rangle$ and $\langle H_0 \rangle_q$ are usually very small. We also do not present the results for $\langle D \rangle$, $\langle P \rangle$, $\langle D \rangle_q$, and $\langle P \rangle_q$ for precessing states since these $\langle A \rangle$'s are very small, and the $\langle A \rangle_q$'s rigorously vanish.

We thus present, in Fig. 4(a), the semiclassical and quantum expectation values of selected properties for states with $n=20$. It is clear that the semiclassical expectation values, open symbols connected by dashed lines, do behave in the qualitative manner anticipated from the earlier discussion. We see that the quantum results also follow the general trends in the $\langle A \rangle$: the $\langle D \rangle_q$ and $\langle P \rangle_q$ decrease from relatively high values as $|l|$ increases, while $\langle L^2 \rangle_q$ increases. $\langle L \rangle_q$ is identically zero for the librating type superpositions, but increases with $|l|$ for the precessing type states. The $\langle A \rangle$ and

$\langle A \rangle_q$ are in good agreement for all of the states with $n=20$, with the sole exception of the state (20,18). Moreover, it may be verified that the relationship $\langle P \rangle \approx \sqrt{3} \langle D \rangle$ is also satisfied by the classical librating-type vague tori. These observations suggest that our procedure is generally successful in generating the correct

quantizing vague tori in the chaotic regime of the Hénon-Heiles system, and also in suppressing, to an appreciable extent, the influence of strong chaos on these vague tori. We postpone to Sec. III B a detailed discussion of the large discrepancies between the $\langle A \rangle$ and $\langle A \rangle_q$, such as observed in the case of state (20,18).

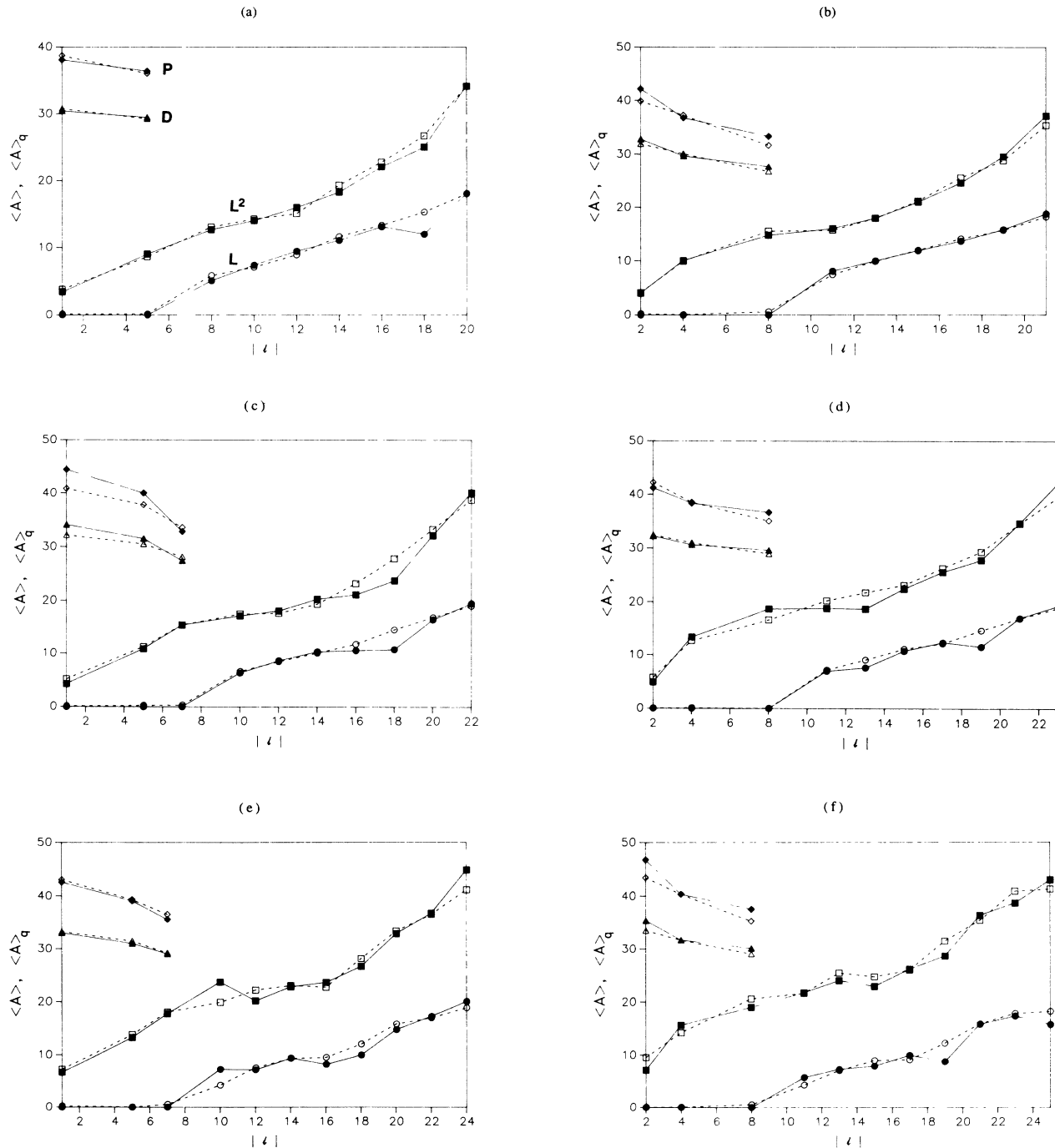


FIG. 4. Quantum and semiclassical expectation values as a function of $|l|$, for states with (a) $n=20$, (b) $n=21$, (c) $n=22$, (d) $n=23$, (e) $n=24$, and (f) $n=25$. The open symbols represent the semiclassical results while the solid symbols represent the corresponding quantum results. Expectation values for L^2 have been multiplied by a factor of 0.1 while the value of 20 has been added to the expectation values for D and P for clarity of presentation. Data are taken from Table II.

TABLE II. Comparison of semiclassical and quantum expectation values. (a) Librating-type states occur in sets of three. The $\langle D \rangle$ and $\langle P \rangle$ that are tabulated correspond to one of these states; the $\langle D \rangle$ and $\langle P \rangle$ for the remaining states can be deduced by symmetry, as described in Ref. 6. (b) Precessing-type states occur in pairs, one having the value of $\langle L \rangle$ that is tabulated and the other having the negative of this value.

State	A	$\langle A \rangle_q$	$\langle A \rangle$	σ_A	μ_A
(a) Librating-type states					
[20,0]	E	19.6343	19.6387	0.0001	0.0005
{40 A_1 , 69 E }	H_0	23.11	22.87	0.35	0.32
	L	0.0	0.17	0.29	0.35
	L^2	34.2	37.9	0.6	1.9
	D	-10.44	-10.78	0.46	0.28
	P	-18.08	-18.69	0.16	0.31
[19,1]	E	19.8420	19.8474	0.0005	0.0006
{31 A_2 , 70 E }	H_0	22.46	22.44	0.26	0.26
	L	0.0	0.17	0.68	0.53
	L^2	90.3	86.4	3.3	4.0
	D	-9.46	-9.27	0.35	0.43
	P	-16.38	-16.05	0.25	0.35
[21,0]	E	20.4754	20.4805	0.0011	0.0007
{44 A_1 , 76 E }	H_0	20.41	24.47	0.05	0.36
	L	0.0	0.23	0.18	0.63
	L^2	40.5	41.1	1.7	2.3
	D	-12.79	-11.90	0.07	0.29
	P	-22.16	-19.88	0.03	0.34
[20,1]	E	20.7080	20.7126	0.0006	0.0007
{33 A_2 , 78 E }	H_0	23.67	23.93	0.28	0.30
	L	0.0	0.07	0.31	0.56
	L^2	100.6	99.6	1.5	4.7
	D	-9.68	-10.08	0.33	0.45
	P	-16.77	-17.24	0.57	0.36
[19,2]	E	20.8687	20.8623	0.0006	0.0007
{45 A_1 , 79 E }	H_0	23.10	22.95	0.12	0.18
	L	0.0	0.62	0.18	0.71
	L^2	148.1	155.7	6.3	5.7
	D	-7.69	-6.73	0.33	0.73
	P	-13.32	-11.66	0.39	0.52
[22,0]	E	21.3206	21.3078	0.0008	0.0009
{47 A_1 , 83 E }	H_0	25.84	25.62	0.24	0.40
	L	0.0	0.12	0.35	0.42
	L^2	42.6	51.6	3.7	2.9
	D	-14.12	-12.19	0.41	0.32
	P	-24.45	-20.86	0.08	0.35
[21,1]	E	21.5622	21.5651	0.0006	0.0011
{37 A_2 , 84 E }	H_0	24.97	24.88	0.15	0.31
	L	0.0	0.25	0.58	0.61
	L^2	108.4	112.3	4.6	5.8
	D	-11.54	-10.51	0.32	0.45
	P	-20.00	-17.83	0.21	0.39
[20,2]	E	21.7425	21.7468	0.0012	0.0010
{49 A_1 , 86 E }	H_0	24.38	24.11	0.13	0.22
	L	0.0	0.31	0.54	0.69
	L^2	154.1	154.1	0.2	6.4
	D	-7.41	-8.12	0.60	0.62
	P	-12.84	-13.61	0.37	0.48
[23,0]	E	22.1151	22.1236	0.0019	0.0012
{51 A_1 , 89 E }	H_0	27.28	27.01	0.62	0.45
	L	0.0	0.05	0.32	0.44

TABLE II. (Continued).

State	A	$\langle A \rangle_q$	$\langle A \rangle$	σ_A	μ_A
	L^2	48.8	57.7	3.9	3.4
	D	-12.24	-12.44	0.42	0.32
	P	-21.21	-22.26	0.44	0.42
[22,1]	E	22.4091	22.4088	0.0003	0.0015
{40 $A_2, 92E$ }	H_0	26.02	25.97	0.27	0.34
	L	0.0	0.12	0.59	0.64
	L^2	133.9	126.7	4.1	5.8
	D	-10.60	-10.97	0.30	0.47
	P	-18.37	-18.54	0.57	0.42
[21,2]	E	22.6154	22.6134	0.0007	0.0014
{54 $A_1, 93E$ }	H_0	25.32	25.66	0.26	0.72
	L	0.0	0.02	0.97	0.71
	L^2	187.0	166.3	0.7	7.9
	D	-9.61	-8.90	0.66	0.64
	P	-16.65	-15.03	0.89	0.53
[24,0]	E	22.9095	22.9244	0.0012	0.0017
{55 $A_1, 95E$ }	H_0	28.54	28.37	0.42	0.49
	L	0.0	0.22	0.27	0.49
	L^2	66.6	72.5	2.3	4.0
	D	-13.04	-13.27	0.39	0.34
	P	-22.59	-23.08	0.38	0.46
[23,1]	E	23.2369	23.2424	0.0015	0.0021
{44 $A_2, 98E$ }	H_0	27.60	27.46	0.17	0.39
	L	0.0	0.04	0.72	0.67
	L^2	132.6	137.9	4.1	8.0
	D	-11.02	-11.49	0.50	0.52
	P	-19.09	-19.33	0.06	0.48
[22,2]	E	23.4643	23.4699	0.0005	0.0020
{57 $A_1, 10E$ }	H_0	27.00	27.01	0.13	0.36
	L	0.0	0.55	0.75	0.77
	L^2	178.0	181.0	10.9	9.0
	D	-9.02	-9.19	0.24	0.66
	P	-15.62	-16.57	0.32	0.57
[25,0]	E	23.6907	23.7103	0.0034	0.00024
{58 $A_1, 104E$ }	H_0	30.20	29.43	0.19	0.51
	L	0.0	0.05	0.24	0.56
	L^2	71.5	95.6	3.3	5.8
	D	-15.46	-13.56	0.06	0.40
	P	-26.79	-23.44	0.20	0.47
[24,1]	E	24.0445	24.0571	0.0031	0.0030
{47 $A_2, 106E$ }	H_0	28.74	29.22	0.32	0.46
	L	0.0	0.07	0.33	0.67
	L^2	156.4	14.20	3.3	8.7
	D	-11.76	-11.74	0.43	0.59
	P	-20.37	-20.36	0.17	0.62
[23,2]	E	24.2907	24.3131	0.0006	0.0029
{61 $A_1, 108E$ }	H_0	28.48	28.45	0.39	0.40
	L	0.0	0.56	1.26	0.81
	L^2	190.0	189.6	2.0	10.3
	D	-10.15	-9.67	0.59	0.80
	P	-17.58	-15.34	0.29	0.69
	(b) Precessing-type states				
(20,8)	E	20.0007	19.9973	0.0009	0.0008
72E	H_0	22.10	22.16	0.16	0.18
	L	5.07	5.86	0.25	0.56

TABLE II. (Continued).

State	A	$\langle A \rangle_q$	$\langle A \rangle$	σ_A	μ_A
	L^2	126.7	130.8	5.4	5.8
(20,10)	E	20.1124	10.1069	0.0007	0.0011
73E	H_0	22.08	21.91	0.10	0.18
	L	7.41	7.11	0.13	0.55
	L^2	140.3	142.8	5.6	7.3
(20,12)	E	20.2589	20.2565	0.0008	0.0010
{43 A_1 , 32 A_2 }	H_0	22.04	21.95	0.04	0.19
	L	9.46	8.92	0.42	0.47
	L^2	159.9	150.9	7.3	8.1
(20,14)	E	20.4401	20.4369	0.0003	0.0010
75E	H_0	22.01	21.90	0.12	0.18
	L	11.09	11.66	0.36	0.44
	L^2	182.8	193.2	11.2	9.5
(20,16)	E	20.6592	20.6567	0.0010	0.0008
77E	H_0	21.80	21.66	0.16	0.16
	L	13.12	13.36	0.05	0.40
	L^2	220.7	228.2	0.2	9.6
(20,18)	E	20.9224	20.9177	0.0003	0.0008
{46 A_1 , 34 A_2 }	H_0	21.78	21.52	0.04	0.15
	L	12.01	15.30	0.13	0.33
	L^2	250.7	267.5	3.1	9.7
(20,20)	E	21.2346	21.2286	0.0005	0.0005
82E	H_0	21.02	21.23	0.03	0.12
	L	18.07	18.02	0.06	0.23
	L^2	341.4	341.2	2.6	8.5
(21,11)	E	21.0557	21.0529	0.0005	0.0011
80E	H_0	23.22	23.33	0.20	0.22
	L	8.12	7.47	0.04	0.57
	L^2	160.7	157.5	3.1	8.0
(21,13)	E	21.2151	21.2124	0.0012	0.0013
81E	H_0	23.20	23.09	0.07	0.21
	L	9.99	9.91	0.53	0.50
	L^2	179.9	179.4	10.0	9.67
(21,15)	E	21.4115	21.4088	0.0001	0.0013
{48 A_1 , 36 A_2 }	H_0	23.06	23.24	0.16	0.22
	L	11.88	11.98	0.42	0.48
	L^2	209.9	211.7	3.8	10.2
(21,17)	E	21.6451	21.6424	0.0009	0.0011
85E	H_0	22.90	22.90	0.19	0.18
	L	13.67	14.14	0.47	0.43
	L^2	245.7	255.3	10.1	10.6
(21,19)	E	21.9247	21.9195	0.0005	0.0010
88E	H_0	22.61	22.51	0.13	0.15
	L	15.87	15.75	0.29	0.37
	L^2	295.6	288.0	6.9	11.2
(21,21)	E	22.2585	22.2519	0.0002	0.0006
{52 A_1 , 39 A_2 }	H_0	22.07	22.27	0.16	0.13
	L	18.80	18.25	0.25	0.26
	L^2	371.5	353.7	9.5	9.8
(22,10)	E	21.8628	21.8538	0.0011	0.0018
87E	H_0	24.29	24.31	0.16	0.24
	L	6.31	6.62	0.56	0.64
	L^2	171.5	174.9	8.6	7.9

TABLE II. (Continued).

State	A	$\langle A \rangle_q$	$\langle A \rangle$	σ_A	μ_A
(22,12)	E	21.9978	21.9966	0.0003	0.0015
{50 A_1 , 38 A_2 }	H_0	24.40	24.12	0.14	0.23
	L	8.63	8.45	0.76	0.59
	L^2	180.7	176.2	8.3	8.8
(22,14)	E	22.1731	22.1670	0.0009	0.0016
90E	H_0	24.36	24.26	0.05	0.23
	L	10.30	10.08	0.42	0.55
	L^2	202.6	193.3	12.9	10.9
(22,16)	E	22.3757	22.3778	0.0007	0.0016
91E	H_0	24.61	24.24	0.04	0.21
	L	10.54	11.74	0.32	0.56
	L^2	210.9	231.8	5.2	11.4
(22,18)	E	22.6202	22.6262	0.0011	0.0014
{53 A_1 , 41 A_2 }	H_0	24.58	23.80	0.02	0.19
	L	10.73	14.53	0.51	0.48
	L^2	237.1	278.2	9.8	11.4
(22,20)	E	22.9249	22.9206	0.0021	0.0013
96E	H_0	23.73	24.00	0.17	0.18
	L	16.44	16.86	0.08	0.40
	L^2	321.3	332.8	1.4	12.4
(22,22)	E	23.2820	23.2736	0.0012	0.0013
99E	H_0	23.15	23.43	0.03	0.15
	L	19.45	19.01	0.12	0.30
	L^2	401.2	387.8	2.5	11.6
(23,11)	E	22.7891	22.7849	0.0012	0.0009
94E	H_0	25.56	25.82	0.13	0.30
	L	6.96	7.17	0.65	0.71
	L^2	188.2	202.2	2.5	9.3
(23,13)	E	22.9467	22.9369	0.0016	0.0020
97E	H_0	25.97	25.39	0.14	0.24
	L	7.60	9.09	0.33	0.65
	L^2	187.1	217.5	5.9	11.0
(23,15)	E	23.1238	23.1203	0.0030	0.0021
{56 A_1 , 43 A_2 }	H_0	25.56	25.87	0.07	0.28
	L	10.76	10.32	0.36	0.59
	L^2	224.3	211.4	3.4	11.8
(23,17)	E	23.3485	23.3452	0.0021	0.0018
100E	H_0	25.42	25.34	0.10	0.22
	L	12.37	12.15	0.49	0.63
	L^2	255.6	262.6	6.36	12.2
(23,19)	E	23.6290	23.6098	0.0086	0.0017
103E	H_0	25.50	24.88	0.05	0.20
	L	11.55	14.67	0.49	0.51
	L^2	277.5	292.9	9.4	13.2
(23,21)	E	23.9233	23.9196	0.0007	0.0017
{60 A_1 , 46 A_2 }	H_0	24.90	24.91	0.09	0.20
	L	17.01	16.94	0.54	0.46
	L^2	346.3	345.47	12.4	14.3
(23,23)	E	24.3046	24.2940	0.0009	0.0013
109E	H_0	24.41	24.61	0.27	0.28
	L	19.29	18.88	0.17	0.35
	L^2	421.5	395.1	7.4	13.3

TABLE II. (Continued).

State	A	$\langle A \rangle_q$	$\langle A \rangle$	σ_A	μ_A
(24,10)	E	23.5883	23.5810	0.0024	0.0030
102E	H_0	26.19	26.61	0.27	0.28
	L	7.22	4.21	0.47	0.75
	L^2	230.7	199.0	3.1	9.6
(24,12)	E	23.7235	23.7165	0.0002	0.0022
{59 A_1 , 45 A_2 }	H_0	27.04	27.12	0.48	0.31
	L	7.13	7.53	0.85	0.73
	L^2	201.5	221.5	8.2	9.5
(24,14)	E	23.8786	23.8764	0.0002	0.0026
105E	H_0	26.79	26.50	0.04	0.26
	L	9.38	9.32	0.66	0.68
	L^2	227.6	229.9	10.1	12.4
(24,16)	E	24.0931	24.0724	0.0011	0.0027
107E	H_0	27.11	27.25	0.16	0.31
	L	8.17	9.52	1.17	0.67
	L^2	236.1	226.9	15.2	11.9
(24,18)	E	24.3299	24.3096	0.0015	0.0023
{62 A_1 , 48 A_2 }	H_0	26.99	26.49	0.05	0.23
	L	9.97	12.03	0.71	0.67
	L^2	265.5	281.1	11.3	12.5
(24,20)	E	24.6027	24.5923	0.0021	0.0020
112E	H_0	26.27	26.16	0.17	0.24
	L	14.76	15.84	0.40	0.54
	L^2	329.2	333.9	9.9	15.0
(24,22)	E	24.9184	24.9161	0.0019	0.0024
115E	H_0	26.14	26.08	0.10	0.21
	L	17.28	16.99	0.04	0.50
	L^2	368.4	365.9	2.8	15.3
(24,24)	E	25.3235	25.3123	0.0025	0.0017
{67 A_1 , 52 A_2 }	H_0	25.57	26.24	0.44	0.20
	L	20.07	18.88	0.44	0.44
	L^2	448.8	411.7	12.5	15.9
(25,11)	E	24.5050	24.4940	0.0002	0.0032
111E	H_0	28.19	28.43	0.09	0.34
	L	5.68	4.28	0.26	0.80
	L^2	217.3	216.3	3.9	11.0
(25,13)	E	24.6448	24.6424	0.0038	0.0028
113E	H_0	27.92	27.48	0.20	0.28
	L	7.26	7.02	0.89	0.84
	L^2	239.7	253.9	11.0	11.9
(25,15)	E	24.8022	24.8126	0.0038	0.0035
{64 A_1 , 50 A_2 }	H_0	28.59	28.43	0.27	0.33
	L	7.91	8.98	0.20	0.74
	L^2	229.1	247.0	5.2	13.2
(25,17)	E	25.023	25.014	0.003	0.004
116E	H_0	28.35	28.56	0.16	0.33
	L	9.96	9.11	0.74	0.76
	L^2	261.5	259.6	10.0	12.5
(25,19)	E	25.2699	25.2759	0.0022	0.0024
119E	H_0	28.23	27.23	0.18	0.23
	L	8.75	12.24	0.49	0.72
	L^2	286.5	315.31	10.9	14.3
(25,21)	E	25.5818	25.5723	0.0012	0.0026
{69 A_1 , 54 A_2 }	H_0	27.34	27.26	0.35	0.26

TABLE II. (Continued).

State	A	$\langle A \rangle_q$	$\langle A \rangle$	σ_A	μ_A
	L	15.80	15.88	0.69	0.60
	L^2	364.3	354.5	15.5	15.7
(25,23)	E	25.9085	25.9089	0.0027	0.0031
125E	H_0	27.49	27.54	0.13	0.24
	L	17.32	17.82	0.16	0.54
	L^2	387.1	409.1	17.8	16.9
(25,25)	E	26.3443	26.3254	0.0036	0.0025
130E	H_0	27.67	27.87	0.22	0.24
	L	15.73	18.20	0.48	0.51
	L^2	430.0	412.8	17.5	18.1

The results for the states with $n = 21, 22, 23, 24,$ and 25 are presented in Figs. 4(b)–4(f), respectively. We see from these figures that the trends in the $\langle A \rangle$ remain essentially unchanged as n increases. The $\langle A \rangle_q$ on average seem to follow the trends in the $\langle A \rangle$, in each of the figures. However, significant deviations from the anticipated behavior are observed in many instances. Also, substantial differences between the $\langle A \rangle$ and the $\langle A \rangle_q$ become more frequent as n increases.

A more complete description of our results is presented in Table II. Also listed in that table are the identities of the states that are combined to form each of the superpositions, and the $(n, |l\rangle)$ or $[n_x, n_y]$ assignments of the superposition states. In addition, two measures of the reliability of the classical calculations are tabulated: (i) standard deviation σ_A in the $\langle A \rangle$ taken over the results of three calculations with $\alpha = 8.0, 10.0,$ and 12.0 ; and (ii) the Monte-Carlo error, given by $\mu_A = \Delta A_{\text{rms}}/N^{1/2}$, where ΔA_{rms} is the rms deviation in $\langle A \rangle$ computed over an ensemble of N trajectories. The Monte Carlo errors μ_A presented in Table II are the largest of the Monte Carlo errors among the calculations for the three values of α . The largest ΔE_{rms} values among the three calculations for a given state is therefore, given by $\Delta E_{\text{rms}} = N^{1/2} \mu_E$.

A review of Table II reveals that the AS energies always agree with the exact quantum superposition energies to within ΔE_{rms} . This is an important finding, since we saw in Sec. II B that the use of the switching function $s(t)$ in AS did not yield the correct quantized energies in the case of the state [22,2]. This also indicates that we have superposed the correct energy eigenstates for our comparison with the AS results. Turning to the standard deviations σ_A , we see that they are almost always quite small compared to the $\langle A \rangle$, indicating that the latter quantities are relatively insensitive to the choice of the parameter α in $s(u)$. In Sec. II B, we interpreted the insensitivity of the $\langle A \rangle$ to the value of α to mean that the vague tori at the end of the switching process are relatively well preserved, and localized in specific regions of phase space. The accuracy of the AS energies and the small values of σ_A therefore indicate that our procedure succeeds in producing quantized vague tori that are relatively free from the influence of chaos.

B. Quantum-classical discrepancies

We consider states for which $|\langle A \rangle - \langle A \rangle_q| > 2\mu_A$ for any A examined as exhibiting a quantum-classical discrepancy. Admittedly, this condition is rather arbitrary and allows a rather generous range of differences to be treated as insignificant. However, it ensures that we will not encounter too many apparent discrepancies that are simply artifacts of the Monte Carlo procedure, and accounts, approximately, for the presence of the standard errors σ_A that are often on the order of the μ_A .

Note that we do not consider the total energy E as one of the properties A while detecting discrepancies by the above procedure. This is because, unlike the remaining properties, the energy is a function only of action variables for an integrable system. As a result, the energy is much less sensitive to differences in the quantum and classical phase-space densities than the other properties. Furthermore, the very small values of the μ_E suggest that these Monte Carlo errors measure only the spread in action variables in the vague torus. Thus violations of the condition $|\langle H \rangle - \langle H \rangle_q| \leq 2\mu_E$ indicate limitations of the classical AS method due to nonadiabaticity and chaos, rather than the essential differences in the quantum and classical state densities that are of primary interest here.

Table III lists the states that exhibit classical-quantum discrepancies, according to the above criterion, and identifies the properties A in which the discrepancies are observed. Such discrepancies can arise from two distinct sources: (i) purely classical effects that cause failure of the AS method to produce accurate vague tori for certain states, and (ii) purely quantum effects that cause actual differences in the forms of the classical and quantum phase space densities for certain states. Discrepancies of the second kind imply differences in the quantum and classical dynamics and are the main subject of concern in this work.

A substantial amount of evidence supports the view that the discrepancies listed in Table III are not caused by the purely classical inadequacy of the AS method to produce vague tori. Such a failure of the AS method could, conceivably, be caused by the chaotic nature of the

final system, or by the passage across separatrices bounding large classical resonant zones^{23,28,29} during the switching process. However, it is unlikely that the presence of chaos is directly responsible for the differences, since states that exhibit the disagreements do not considerably lie in the most chaotic regions of phase space. Indeed, there are states in highly chaotic portions of phase space that do not show significant classical-quantum discrepancies. Also, it does not appear that the passage across separatrices causes the differences. This may seem to be an especially likely source of the discrepancies since (as we will show below) many such discrepancies are associated with avoided crossings of quantum energy level curves near $\lambda=0.08$, and such crossings are known to indicate the existence of classical resonance conditions.^{29,47-52} However, if this were indeed the source of the discrepancies, we would expect them to be accompanied by especially large values of ΔE_{rms} , indicating strong nonadiabaticities—an effect that is not observed. In addition, if this were the cause of the differences, we would expect to find quantum-classical disagreements for all precessing states with levels that undergo avoided crossings with $\lambda < 0.08$, not just those that have crossings at $\lambda \approx 0.08$. This, again is not observed. Our conclusion that the resonances are ineffective in causing the discrepancies is consistent with their weak and high-order nature.^{23,28}

Figure 4 provides additional evidence that the discrepancies are not due to purely classical effects that cause the AS method to fail for certain states. It is evident from these figures that, in most cases, the discrepan-

cies are accompanied by strong irregularities in the *quantum*—not the classical—curves. This suggests that the disagreements result from effects that occur in the quantum calculations for specific states, i.e., that the discrepancies signify true differences between the quantum and classical descriptions of the states. Additional evidence that the discrepancies are associated with quantum effects will be presented later in this section.

We now attempt to identify the quantum effects that cause the discrepancies. As we describe below, it is possible to attribute almost all of the quantum-classical disagreements to two quantum phenomena: trapping effects that occur for states with extreme values for quantum numbers and nonclassical effects that are associated with avoided crossings (AC's) of energy levels as a function of the parameter λ .

Quantum-mechanical trapping^{53,54} is a localization of states in regions of phase space associated with extreme values for quantum numbers, when the classical system displays no such behavior. Trapping has, by now, been observed in a variety of systems,⁵³⁻⁵⁹ including the present one.⁶ It can be explained in several (possibly equivalent) ways as being caused by the ineffectiveness in quantum systems of narrow, high-order classical resonances,⁵³ certain nonadiabatic effects,⁵⁸ or low classical flux through barriers (the quantum suppression of chaos^{2,3,5}). For the Hénon-Heiles system with energy near the dissociation limit, trapping occurs for two kinds of states:⁵⁶ states $[n_x, n_y]$ with low n_y (especially $n_y=0$), and states (n, l) with high l (especially $l=n$). The localized nature of quantum states relative to their classical counterparts leads to the following predictions⁶ for the expectation values $\langle A \rangle$:

$$\langle L^2 \rangle_q < \langle L^2 \rangle, \langle D \rangle_q > \langle D \rangle, \langle P \rangle_q > \langle P \rangle, \text{ low } n_y$$

$$\langle L^2 \rangle_q > \langle L^2 \rangle, \langle L \rangle_q > \langle L \rangle, \text{ high } l.$$

Table III identifies those discrepancies that are due to trapping. It can be verified that the anticipated effects on the $\langle A \rangle$ are indeed observed in most cases. However, exceptions occur for states [23,0] and (25,25). The exception for [23,0] may be due to the influence of weak AC's which tend to oppose the effects of trapping on the expectation values. As shown below, the simultaneous action by trapping and AC effects also explains the absence of discrepancies for state [24,0] which would be expected to show a strong trapping influence. The exception for (25,25) may be related to the fact that this state lies above the dissociation energy for the system.

Almost all of the remaining discrepancies listed in Table III can be associated with avoided crossings of energy eigenvalues near $\lambda=0.08$. To make this matter clearer, Fig. 5 shows a range of Hénon-Heiles energy levels as a function of λ , between $\lambda=0.075$ and 0.085. Those avoided crossings in this energy range that are associated with nontrapping quantum-classical discrepancies are marked by circles placed at the closest approach of the energy levels. It is immediately apparent that all such AC's occur near $\lambda=0.08$, while states that undergo avoided crossings away from $\lambda=0.08$ do not show such discrepancies. This finding has the following significance.

TABLE III. Discrepancies between quantum and classical expectation values.

State	Discrepant properties ^a	Explanations
Librating-type states		
[21,0]	$\langle D \rangle_q, \langle P \rangle_q$	trapping
[19,2]	$\langle P \rangle_q$	AC: (21,9)-(20,18)
[22,0]	$\langle L^2 \rangle, \langle D \rangle_q, \langle P \rangle_q$	trapping
[21,1]	$\langle D \rangle_q, \langle P \rangle_q$	unknown
[23,0]	$\langle L^2 \rangle, \langle P \rangle$	trapping
[21,2]	$\langle L^2 \rangle_q, \langle P \rangle_q$	AC: (23,9)-(22,18)
[25,0]	$\langle L^2 \rangle, \langle D \rangle_q, \langle P \rangle_q$	trapping
[23,2]	$\langle P \rangle_q$	AC: (25,9)-(24,18)
Precessing-type states		
(20,18)	$\langle L \rangle$	AC: (21,9)-(20,18)
(22,16)	$\langle L \rangle$	AC: (23,5)-(22,16)
(22,18)	$\langle H_0 \rangle_q, \langle L \rangle, \langle L^2 \rangle$	AC: (23,9)-(22,18)
(23,13)	$\langle H_0 \rangle_q, \langle L \rangle, \langle L^2 \rangle$	AC: (24,2)-(23,13)
(23,19)	$\langle H_0 \rangle_q, \langle L \rangle$	AC: (24,10)-(23,19)
(24,10)	$\langle L \rangle_q, \langle L^2 \rangle_q$	AC: (24,10)-(23,19)
(24,12)	$\langle L^2 \rangle$	AC: (25,3)-(24,12)
(24,16)	$\langle L \rangle$	AC: (25,5)-(24,16)
(24,18)	$\langle H_0 \rangle_q, \langle L \rangle$	AC: (25,9)-(24,18)
(24,24)	$\langle H_0 \rangle, \langle L \rangle_q, \langle L^2 \rangle_q$	trapping
(25,19)	$\langle H_0 \rangle_q, \langle L^2 \rangle, \langle L \rangle$	AC: (26,10)-(25,19)
(25,25)	$\langle L \rangle$	trapping

^aThe larger of $\langle A \rangle$ and $\langle A \rangle_q$ is listed.

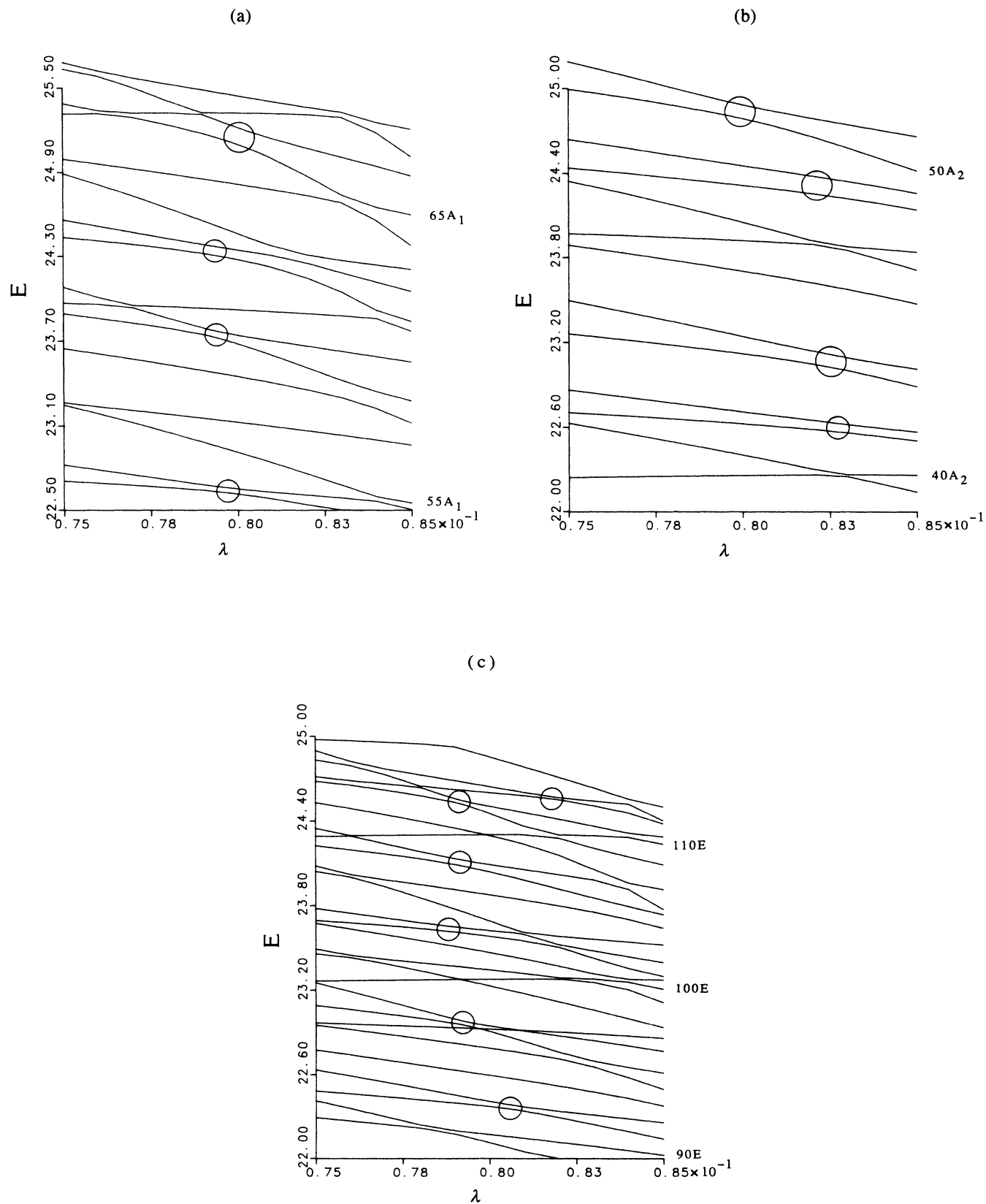


FIG. 5. Some energy eigenvalues of the Hénon-Heiles system as a function of λ for the range $0.075 \leq \lambda \leq 0.085$. Avoided crossings with $R(0.08) > 0.6$ are circled. (a) States of A_1 symmetry, (b) states of A_2 symmetry, (c) states of E symmetry.

TABLE IV. Avoided crossings in the Hénon-Heiles system for the range $0.075 \leq \lambda \leq 0.085$ and $17.9 \leq E \leq 25.3$

States ($n, l $)-($n', l' $)	$R(0.08)$	Δ	λ_x
(18,0)-(17,15)	0.49	0.004	0.0802
(20,0)-(19,15)	0.28	0.011	0.079
(22,0)-(21,15)	0.11	0.012	0.077
(24,0)-(23,15)	0.08	0.017	0.075 ^a
(19,1)-(18,14)	0.11	0.011	0.0833 ^b
(21,1)-(20,14)	0.37	0.013	0.0810 ^b
(23,1)-(22,14)	0.29	0.017	0.0785 ^b
(25,1)-(24,14)	0.10	0.109	0.0760 ^b
(19,1)-(18,16)	0.06	0.009	0.076 ^c
(21,1)-(20,16)	0.09	0.016	0.075 ^c
(23,1)-(21,19)	0.06	0.011	0.083 ^c
(25,1)-(23,19)	0.23	0.015	0.081 ^c
(26,2)-(25,11)	0.52	0.026	0.0791
(22,2)-(21,13)	0.10	0.009	0.0810
(24,2)-(23,13)	0.69	0.027	0.0793
(26,2)-(25,13)	d	0.032	0.076
(22,2)-(20,20)	0.06	0.004	0.0812
(24,2)-(22,20)	0.10	0.002	0.0797
(26,2)-(24,20)	0.10	0.009	0.078
(26,2)-(23,23)	0.15	0.023	0.082
(23,3)-(22,12)	0.41	0.049	0.0826 ^{c,e}
(25,3)-(24,12)	0.75	0.046	0.0792 ^{c,e}
(23,3)-(21,21)	0.08	0.011	0.078 ^f
	0.09	0.013	0.083
(25,3)-(23,21)	0.52	0.126	0.077 ^f
	0.20	0.026	0.082
(18,4)-(17,17)	0.09	0.008	0.0766 ^a
(20,4)-(19,17)	0.05	0.004	0.077 ^a
(22,4)-(21,17)	0.11	0.010	0.077 ^a
(24,4)-(23,17)	0.14	0.016	0.076 ^a
(24,4)-(22,22)	0.06	0.003	0.0791
(26,4)-(24,22)	0.39	0.025	0.0793
(17,5)-(16,16)	0.07	0.004	0.082
(19,5)-(18,16)	0.21	0.012	0.082 ^a
(21,5)-(20,16)	0.33	0.017	0.082 ^a
(23,5)-(22,16)	0.82	0.030	0.0808
(25,5)-(24,16)	0.80	0.042	0.0793 ^a
(22,6)-(21,15)	0.45	0.071	0.085 ^g
(24,6)-(23,15)	0.73	0.089	0.083 ^g
(26,6)-(25,15)	1.00	0.098	0.0799 ^g
(25,7)-(23,23)	0.40	0.003	0.0799 ^c
(25,7)-(24,16)	0.22	0.045	0.084 ^c
(18,8)-(17,17)	0.22	0.013	0.082 ^a
(20,8)-(19,17)	0.25	0.021	0.084 ^a
(22,8)-(21,17)	0.43	0.047	0.085 ^a
(24,8)-(23,17)	0.51	0.063	0.083
(24,8)-(22,22)	0.11	0.021	0.084
(19,9)-(18,18)	0.19	0.005	0.0790 ^f

TABLE IV. (Continued).

States ($n, l $)-($n', l' $)	$R(0.08)$	Δ	λ_x
	0.38	0.005	0.0795
(21,9)-(20,18)	0.84	0.016	0.0796 ^f
	0.63	0.200	0.0810
(23,9)-(22,18)	0.99	0.037	0.0797 ^f
	0.70	0.059	0.084
(25,9)-(24,18)	0.93	0.063	0.0791 ^f
	0.82	0.118	0.085
(20,10)-(19,19)	0.10	0.010	0.076 ^a
(22,10)-(21,19)	0.26	0.016	0.077 ^a
(24,10)-(23,19)	0.87	0.035	0.0790 ^a
(26,10)-(25,19)	1.00	0.073	0.0803 ^a
(23,11)-(22,20)	0.34	0.040	0.083
(25,11)-(23,23)	0.15	0.030	0.084 ^c
(26,12)-(25,21)	0.16	0.021	0.075 ^{b,c}
(26,12)-(24,24)	0.31	0.037	0.083 ^f
	0.36	0.019	0.0809
(21,13)-(20,20)	0.02	0.001	0.0793
(23,13)-(22,20)	0.09	0.002	0.0809
(25,13)-(24,20)	0.34	0.014	0.082
(24,16)-(23,23)	0.02	0.003	0.076 ^c
(23,17)-(22,22)	0.13	0.009	0.082
(25,17)-(24,22)	0.17	0.018	0.082

^aThe $|l'|$ state is involved in more than one isolated avoided crossing for the range of λ considered.

^bThe $|l|$ state is involved in more than one isolated avoided crossing for the range of λ considered.

^cBoth states are involved in more than one isolated avoided crossing for the range of λ considered.

^d $R(0.08)$ not computed since other AC's intervene between λ_x and 0.08.

^eOnly the A_1 states are involved in the avoided crossing.

^fBoth the A_1 and A_2 states are involved in the avoided crossing. The value for the A_1 state is reported on the first line, and that for the A_2 state, on the second.

^gOnly the A_2 states are involved in the avoided crossing.

If the avoided crossings were associated with classical resonances, and the discrepancies were due to the breakdown of the AS method at sufficiently strong resonances, we would expect the discrepancies to be present in every case the states are involved in an avoided crossing for $\lambda \leq 0.08$, not just those that take place near $\lambda = 0.08$. Figure 5, therefore, suggests that a *nonclassical* phenomenon is associated with the circled AC's, which in turn are responsible for the observed quantum-classical discrepancies.

To quantify the effects of the AC's on the expectation values, we introduce three parameters to describe each such AC. Consider an avoided crossing between two energy curves $E_+(\lambda)$ and $E_-(\lambda)$. Then λ_x , the values of λ at the AC, is defined as the λ for which $|E_+(\lambda) - E_-(\lambda)|$ is a minimum. The splitting Δ is defined as

$$\Delta = |E_+(\lambda_x) - E_-(\lambda_x)|, \quad (14)$$

while the ratio $R(\lambda)$ is defined as

$$R(\lambda) = \Delta / |E_+(\lambda) - E_-(\lambda)|. \quad (15)$$

These parameters can be interpreted in a straightforward manner when the AC can be treated as a textbook two-level problem.⁶⁰ Then the energy curves are given by the expression

$$E_{\pm}(\lambda) = \frac{1}{2}[E_1(\lambda) + E_2(\lambda)] \pm \frac{1}{2}\{[E_1(\lambda) - E_2(\lambda)]^2 + 4W_{12}^2\}^{1/2}, \quad (16)$$

where E_1 and E_2 are the two uncoupled diabatic energy curves that cross at λ_x , and W_{12} is the effective interaction which perturbs the states and which is assumed here to be roughly constant in the vicinity of λ_x . Let us denote the eigenfunctions associated with E_{\pm} by ψ_{\pm} and the diabatic states associated with energies E_j and ϕ_j , so that

$$\psi_{\pm}(\lambda) = C_{\pm 1}(\lambda)\phi_1 + C_{\pm 2}(\lambda)\phi_2. \quad (17)$$

TABLE V. Expectation values for diabatic states formed from energy eigenstates involved in avoided crossings.

State	A	$\langle A \rangle_q$ (adiabatic) ^a	$\langle A \rangle^b$	μ_A	$\langle A \rangle_q$ (diabatic) ^c
AC: (24,2)-(23,13), 95E-97E ($R=0.69$)					
[24,0]	E	22.9095	22.9244	0.0017	22.9131
{55 A_1 , 95E}	H_0	28.54	28.37	0.49	28.86
	L^2	66.6	72.5	4.0	52.5
	D	-13.04	-13.27	0.33	-15.58
	P	-22.89	-23.08	0.46	-26.97
(23,13)	E	22.9467	22.9396	0.0020	22.9413
97E	H_0	25.95	25.39	0.24	25.49
	L	7.60	9.09	0.64	9.15
	L^2	187	217	11	208
AC: (25,3)-(24,12), 58 A_1 -59 A_1 ($R=0.76$)					
[25,0]	E	23.6907	23.7103	0.0024	23.6941
{58 A_1 , 104E}	H_0	30.20	29.43	0.51	30.44
	L^2	71.5	95.6	5.8	62.4
	D	-15.46	-13.56	0.40	-16.30
	P	-26.79	-23.44	0.47	-28.24
(24,12)	E	23.7235	23.7165	0.0022	23.7184
{59 A_1 , 45 A_2 }	H_0	27.04	27.12	0.31	26.68
	L	7.13	7.53	0.73	7.78
	L^2	201.5	221.5	9.5	215.2
AC: (23,5)-(22,16), 92E-91E ($R=0.82$)					
[22,1]	E	22.4091	22.4088	0.0015	22.4039
{40 A_2 , 92E}	H_0	26.02	25.97	0.34	26.31
	L^2	133.9	126.7	5.8	117.1
	D	-10.60	-10.97	0.47	-10.48
	P	-18.37	-18.54	0.42	-18.15
(22,16)	E	22.3757	22.3778	0.0016	22.3834
91E	H_0	24.61	24.24	0.21	24.17
	L	10.54	11.74	0.56	11.76
	L^2	210.9	231.8	11.4	236.1
AC: (25,5)-(24,16), 106E-107E ($R=0.81$)					
[24,1]	E	24.0445	24.0571	0.0030	24.0513
{47 A_2 , 106E}	H_0	28.74	29.22	0.46	29.07
	L^2	156.4	142.0	8.7	142.2
	D	-11.76	-11.74	0.59	-12.19
	P	-20.37	-20.36	0.62	-21.12
(24,16)	E	24.0931	24.0724	0.0027	24.0828
107E	H_0	27.11	27.25	0.31	27.50
	L	8.17	9.52	0.67	8.23
	L^2	236.1	226.9	11.9	213.7
AC: (24,6)-(23,15), 44 A_2 -43 A_2 ($R=0.73$)					
[23,1]	E	23.2369	23.2424	0.0021	23.2304
{44 A_2 , 98E}	H_0	27.60	27.46	0.39	27.72
	L^2	132.6	137.9	8.0	126.0
	D	-11.02	-11.49	0.52	-11.30
	P	-19.09	-19.33	0.48	-19.58
(23,15)	E	23.1238	23.1203	0.0021	23.1334
{56 A_1 , 43 A_2 }	H_0	25.56	25.87	0.28	25.38
	L	10.76	10.32	0.59	11.19
	L^2	224.3	211.4	11.8	234.3

TABLE V. (Continued).

State	A	$\langle A \rangle_q$ (adiabatic) ^a	$\langle A \rangle^b$	μ_A	$\langle A \rangle_q$ (diabatic) ^c
AC: (26,6)–(25,15), $51 A_2 - 50 A_2$ ($R=1.00$)					
(25,15)	E	24.8022	24.8126	0.0035	24.8268
{64 A_1 , 50 A_2 }	H_0	28.59	28.43	0.33	27.79
	L	7.91	8.98	0.74	10.27
	L^2	229.1	247.0	13.2	264.0
AC's: (21,9)–(20,18), $45 A_1 - 46 A_1$ ($R=0.84$) and $35 A_2 - 34 A_2$ ($R=0.53$)					
[19,2]	E	20.8687	20.8623	0.0007	20.8702
{45 A_1 , 79 E }	H_0	23.10	22.95	0.18	22.80
	L^2	148.1	155.7	5.7	151.2
	D	-7.69	-6.73	0.73	-6.56
	P	-13.32	-11.66	0.52	-11.35
(20,18)	E	20.9224	20.9177	0.0008	20.9219
{46 A_1 , 34 A_2 }	H_0	21.78	21.52	0.15	21.78
	L	12.01	15.30	0.33	15.46
	L^2	250.7	267.5	9.7	278.9
AC's: (23,9)–(22,18), $54 A_1 - 53 A_1$ ($R=0.99$) and $42 A_2 - 41 A_2$ ($R=0.70$)					
[21,2]	E	22.6154	22.6134	0.0014	22.6081
{54 A_1 , 93 E }	H_0	25.32	25.66	0.72	25.69
	L^2	187.0	166.3	7.9	163.7
	D	-9.61	-8.90	0.64	-8.30
	P	-16.65	-15.03	0.53	-14.38
(22,18)	E	22.6202	22.6262	0.0014	22.6341
{53 A_1 , 41 A_2 }	H_0	24.58	23.80	0.19	24.06
	L	10.73	14.53	0.48	14.27
	L^2	237.1	278.2	11.4	265.2
AC's: (25,9)–(24,18), $61 A_1 - 62 A_1$ ($R=0.93$) and $49 A_2 - 48 A_2$ ($R=0.83$)					
[23,2]	E	24.2907	24.3131	0.0029	24.3064
{61 A_1 , 108 E }	H_0	28.48	28.45	0.40	28.70
	L^2	190.0	189.6	10.3	175.8
	D	-10.15	-9.67	0.80	-8.24
	P	-17.58	-15.34	0.69	-14.27
(24,18)	E	24.3299	24.3096	0.0023	24.3218
{62 A_1 , 48 A_2 }	H_0	26.99	26.49	0.23	26.62
	L	9.97	12.03	0.67	12.33
	L^2	265.5	281.1	12.5	269.0
AC: (24,10)–(23,19), $102 E - 103 E$ ($R=0.87$)					
(24,10)	E	23.5883	23.5810	0.0030	23.5986
102 E	H_0	26.19	26.61	0.28	26.59
	L	7.22	4.21	0.75	3.78
	L^2	230.7	199.0	9.6	205.6
(23,19)	E	23.6290	23.6098	0.0017	23.6187
103 E	H_0	25.50	24.88	0.20	25.10
	L	11.55	14.67	0.51	14.99
	L^2	277.5	292.9	13.2	302.5
AC: (26,10)–(25,19), $120 E - 119 E$ ($R=0.69$)					
(25,19)	E	25.2699	25.2759	0.0024	25.3043
119 E	H_0	28.23	27.23	0.23	27.57
	L	8.75	12.24	0.72	13.55
	L^2	286.5	315.31	14.3	324.5

^aQuantum expectation values for ordinary adiabatic states from Table II.

^bSemiclassical expectation values from Table II.

^cQuantum expectation values for the diabatic states obtained as superpositions of the adiabatic states, as described in the text.

Then, it is then easy to show that

$$\Delta = 2W_{12} \quad (18)$$

and

$$R(\lambda) = \{1 - [2C_{\pm j}^2(\lambda) - 1]^2\}^{1/2}, \quad (19)$$

for any of the four values $C_{\pm j}(\lambda)$. Thus Δ measures the strength of the perturbing interaction while $R(\lambda)$ measures the effectiveness of this interaction at mixing the diabatic states at λ .

In order for the two-level model to be valid, the AC must be *isolated*. An AC at λ_x will be isolated if $R(\lambda_x)$ is suitably small for all other AC's that involve either of the levels $E_+(\lambda)$ or $E_-(\lambda)$. A reasonable practical criterion for smallness is $R < 0.6$ since this implies that $C_{\pm j}^2 < 0.1$ or > 0.9 . By these standards, all of the AC's in Fig. 5 may be classified as isolated.

Values of λ_x , Δ , and $R(0.08)$ are presented in Table IV for AC's in the range $0.075 \leq \lambda \leq 0.085$ and $17.9 \leq E \leq 25.3$. AC's with $R(0.08) \geq 0.6$ [i.e., those that yield $0.9 \geq C_{\pm j}^2(0.08) \geq 0.1$] are correlated with several classical-quantum discrepancies in Table III. With only one exception (out of 14 cases), each nontrapping discrepancy is found to be associated with an AC having $R(0.08) \geq 0.6$. Furthermore, with two exceptions (out of 14 cases), all AC's with $R(0.08) \geq 0.6$ are observed to cause discrepancies in at least one of the two states involved. Thus, to summarize our results, of the 60 states examined, 20 are found to show classical-quantum discrepancies. Of these discrepancies, 6 are attributed to trapping, 13 are associated with AC's, and 1 remains unexplained.

To verify that the AC's are indeed responsible for the discrepancies, we calculate quantum expectation values of the properties A for the *adiabatic* states ϕ_j of Eq. (17), using the values of $R(0.08)$ in Table IV to determine the $C_{\pm j}(0.08)$ [see Eq. (19)]. A comparison of these expectation values to the classical $\langle A \rangle$ is presented in Table V. This comparison shows that the formation of the diabatic states eliminates the quantum-classical discrepancies in all cases where Table III attributes these discrepancies to AC's. This convincingly demonstrates that the AC discrepancies are not caused by the purely classical failure of the AS method as the result of chaos or separatrix crossing, but stem from the presence of nonclassical effects.

Note that the formation of diabatic states does not reduce, but actually enhances the quantum-classical discrepancies for states involved in trapping such as [24,0] and [25,0]. Indeed, it creates a discrepancy for the state [24,0] where none had existed before, thus revealing the anticipated trapping nature of this state.

We mentioned earlier that the mixing of character among diabatic states that accompanies the AC's causes a fundamental uncertainty in the assignment of quantum numbers to these states. The present results show, however, that this uncertainty is but a symptom of an underlying quantum effect which ruins the classical-quantum correspondence and brings about the discrepancies. These discrepancies are not caused by the uncertainty in

the assignments and cannot be removed by reassignment of quantum numbers.

In agreement with previous work,^{51,61-67} we identify the nonclassical effect that accompanies AC's as a form of tunneling between (vague) tori. There is much evidence for this interpretation. It is known that primitive semiclassical methods do not prevent energy levels from crossing as a parameter is varied.^{61,62,68} Since the improvements^{51,61,62,67,69} in the semiclassical theory required to cause the curves avoid each other and produce the correct splittings are of the kind needed to treat ordinary tunneling, it is natural to classify AC's as tunneling phenomena. In addition, since the interacting states typically are characterized by different sets quantum numbers (usually association with disjoint parts of phase space) the quantum phenomenon has been identified as tunneling between different tori.^{45,65} We note that the association of AC's with nonclassical phenomena has been most firmly established for sharp AC's that produce small splittings. Our work provides evidence that this association remains valid for gradual AC's that yield splittings on the order of the mean energy spacing (see Fig. 5).

Table III shows that the proportion of states influenced by tunneling increases with the energy (and with the chaotic nature) of the classical system. The number of states involved in strong AC's ($R > 0.6$) grows from two, for $n=20,21$, to eight, for $n=24,25$. This trend is consistent with the data presented in Table IV which organizes AC's into "families" associated with specific pairs (l, l') of l quantum numbers for the participating states. Within almost every family, λ_x varies monotonically and Δ increases monotonically as the energy increases. Exceptions to this trend for Δ are probably due to the difficulty of measuring small splittings accurately. The regularity of the progressions is a consequence of the association of all members of a family with specific classical resonance condition. However, the relevant point here is that, as Δ increases, the range of λ for which $R(\lambda)$ is large increases, and thus more states become influenced by tunneling. At the same time, since the rate of tunneling is proportional to Δ , this rate also increases. Thus, for our system, tunneling becomes more prevalent and faster, causing quantum-classical discrepancies to become more common and more pronounced, as the energy increases.

C. Implications for tunneling in other chaotic systems

Increases in AC level splittings Δ , similar to those observed for our case, have been noted in many other systems as the energy is raised or as the classical motion becomes more chaotic.^{1(b),70-73} This phenomenon has, in fact, been identified as a symptom of chaos^{47-50,52,71,73,74} and has been used^{1(b),52,71,73} to explain the success of the Wigner distribution^{73,75,76} in modeling the statistics of nearest-neighbor energy-level spacings for chaotic systems. We note that many of the AC's appearing in the published plots of the energy-level curves for these cases are similar to those in our calculations. Just as for our system, these AC's are often gradual and lead to splittings on the order of the mean level spacing. Although

not all such AC's are isolated, a substantial proportion of them often are, just as for our system.

Since the AC's in our system are found to imply nonclassical effects, the suspicion arises that the AC's in other chaotic systems may likewise signify tunneling. There is, in fact, evidence that this is true. Davis⁸ and, more recently, Eckhardt, Hose, and Pollak⁷⁷ have noted certain pairs of states in chaotic systems which, when added and subtracted, yield new states describing clearly identifiable classical behavior. This is consistent with the existence of AC's with $R \approx 1$ which induce tunneling. Robnik⁷¹ has examined how the wave functions of a chaotic system change as a parameter in the Hamiltonian varies and AC's are encountered. The mixing of states and the exchange of identities of states that the observes appear to be totally consistent with the mechanism for quantum-classical discrepancies for our system. Radons, Geisel, and Rubner^{3(b)} have attributed enhanced tunneling probabilities for the periodically kicked planar rotor to avoided crossings in the quasienergy spectrum.

If many AC's in other chaotic systems indeed signify tunneling, then the increased occurrence of tunneling observed in our system as it becomes more chaotic is but an example of a more general phenomenon; i.e., tunneling *generally* becomes more prevalent and faster as a system becomes more chaotic. As we will discuss below, this has serious implications for the achievement of statistical behavior in quantum systems.

We note, however, that this interpretation conflicts with an implicit assumption in the literature which associates AC's in chaotic systems with the purely classical-state mixing⁹ that is expected to accompany chaos. This classical interpretation is consistent with the belief that chaotic systems display Wigner nearest-neighbor spacing statistics in the classical limit. Indeed, if the AC's of chaotic systems are symptoms of tunneling, as they are in the case of regular systems,⁶⁶ then the splittings Δ should decrease with \hbar as $\exp(-S/\hbar)$ where $S > 0$, and become negligible compared to mean level separations in the classical limit. Thus, if such AC's are the major source of level repulsions in chaotic systems as $\hbar \rightarrow 0$,⁵² the levels of such systems cannot obey Wigner statistics in the classical limit.

However, since our work does not examine the classical limit, we must be cautious about drawing conclusions concerning the interpretation of AC's or the validity of Wigner statistics for chaotic systems in that limit. For example, it may well be that distinct AC's (i.e., well-defined approaches and avoidances of energy levels as a function of a parameter in the Hamiltonian) no longer occur for chaotic systems in the classical limit. Alternatively, such AC's may still occur but may indeed correspond to classical-state mixing for sufficiently small \hbar . However, in order for these AC's to signify classical-state mixing, it is not sufficient for the individual underlying quantum resonances to behave classically (i.e., for many levels to lie within the resonance widths^{50,53}), since the AC's produced by isolated classical resonances continue to signify tunneling even in the classical limit.⁵¹ The condition for the AC's to represent classical-state mixing would thus have to be connected with the chaotic nature

of the system, i.e., with the overlap of resonances,⁷⁸ perhaps as reflected in the overlap of AC's.^{50,79} We cannot, therefore, rule out the possibility that certain overlapping AC's in published plots of energy eigenvalues are associated with purely classical behavior. However, a sizable proportion of AC's in these plots are isolated and it appears unlikely that AC's would suddenly acquire a classical interpretation as soon as they begin to overlap. Thus the suspicion remains that many of the AC's for other systems—overlapping as well as isolated—signify nonclassical effects, as they do for our system.

It remains to be rationalized how an increased degree of chaos can cause tunneling to become more prevalent and rapid. One explanation begins by recognizing that each AC is associated with a particular classical resonance condition.^{50,52} The energy levels affected by this resonances are determined by solving the Schrödinger equation (subject to appropriate boundary conditions⁵¹) for the rotor system described by the Hamiltonian⁷⁸ $H = p^2/2m + V_0 \cos(2\phi)$. This results in pairs of levels with $E > V_0$,^{51,69} which undergo AC's as a parameter in the original Hamiltonian is varied and which correspond to states of the original system that undergo tunneling. The splitting between these levels can be approximated semiclassically⁶⁹ as $\Delta = 4\hbar\tau^{-1}e^\theta$, where τ is the classical period for rotation by the rotor and e^θ is the amplitude for reflection of waves over the cosine barrier. As the width of the resonance increases, V_0 increases, causing the well to become deeper, and the barrier to become sharper. At a fixed energy above the barrier, the deepening of the well should cause the period of rotation to decrease somewhat and the sharpening of the barrier should cause the reflection amplitude to increase rapidly.⁸⁰ As a result, the splittings associated with tunneling should increase dramatically as the resonance becomes broader. Numerical calculations by Sibert, Hynes, and Reinhardt⁶⁹ conform these expectations. Broadening of resonances also brings about chaos by causing resonances to overlap,⁷⁸ so that one may expect increased degrees of chaos to be accompanied by increased level splittings associated with tunneling.

D. Implications for statistical behavior in quantum systems

From our viewpoint, the most interesting aspects of the results presented here are connected with the purely quantum nature of the tunneling phenomenon, its prevalence in chaotic systems, and the limitations that this imposes on the ability of the quantum systems to imitate the dynamical evolution of their classical counterparts. One type of dynamical behavior that is characteristic of classical chaotic systems and that is strongly relevant to chemical physics is what we have termed pseudoergodicity.^{6,7,44} This is a temporary, approximate form of statistical behavior that can be achieved in phase-space regions which are bounded by bottlenecks impeding the flow of density, such as cantori and separatrices. The importance of pseudoergodicity stems from its relation to refined statistical theories for chemical reactions³³⁻³⁷ and its theoretical significance as the forerunner to global statistical behavior on the full energy shell.

The quantum analog of pseudoergodicity⁴⁴ can be defined and such behavior is expected to appear in the quantum counterparts of chaotic systems, provided that the time scale for quantum-classical correspondence is sufficiently long.^{6,7,44} However, tunneling limits this time scale. When tunneling is fast enough to compete with the classical rate of statistical relaxation within bottlenecked regions, pseudoergodicity cannot occur in the quantum system. In such cases, there can certainly be no analog in the quantum system of the more global behavior that arises at longer times from the classical penetration of bottlenecks.

In previous work,⁶ the pseudoergodicity behavior of the quantum and classical analogs of the Hénon-Heiles system was examined. It was found that the pseudoergodicity behavior of the classical system was often absent in the quantum analog. This was attributed to tunneling and trapping. In fact, the states for which discrepant classical and quantal statistical behavior was observed are just the states shown here to be involved in tunneling and trapping (with allowances for some different assignments⁴⁴ of quantum numbers which, in part, are due to the use of a larger basis in the present calculation).

The arguments presented here imply that increasing degrees of chaos are generally accompanied in a quantum system by more rapid tunneling. If this is the case, statistical behavior is generally hard to achieve in quantum systems because chaos—the condition that makes such behavior possible in classical systems—causes effects that prevent similar behavior from appearing in the quantum analogs.

IV. SUMMARY

We have developed an accelerated AS method that makes it possible to calculate semiclassical expectation values for chaotic systems. To maintain low degrees of nonadiabaticity while preserving the integrity of vague tori, the perturbation is switched on slowly over the regular regime but more rapidly over the chaotic regime. Comparison of the semiclassical results to accurate quantum expectation values yields good agreement for most

high-energy states of the Hénon-Heiles system. However, the frequency of the discrepancies is found to grow with energy. Evidence suggests that these differences are not caused by the failure of the adiabatic switching method to describe vague tori as a result of classical nonadiabaticity or chaos, but are symptoms of purely quantum phenomena. We are able to attribute almost all cases of quantum-classical discrepancies to two such phenomena: trapping effects for states with extreme values for quantum numbers and tunneling effects associated with avoided crossings. As the energy is raised and the system becomes more chaotic, the increased strength of the avoided crossings is found to lead to more frequent and stronger tunneling.

The correlation observed between AC's and quantum effects seems to conflict with the assumption, implicit in much recent work, that gradual AC's which cause large splittings in chaotic systems arise from the classical mixing of states that expected to accompany chaos. Our results show that such AC's can signify nonclassical effects just as do the sharp, narrowly avoided AC's typical of regular systems. However, this does not contradict the claim that AC's generally tend to become broader and stronger as systems become more chaotic, since higher degrees of chaos can lead to stronger tunneling. If a substantial proportion of the robust AC's that accompany chaos in other systems are indeed caused by tunneling, then (i) more frequent and rapid tunneling may generally accompany the onset of chaos in quantum systems, (ii) this rapid tunneling may compete with classical-like relaxation, making it difficult for quantum systems to display even transient statistical behavior, and (iii) this tunneling may be partly responsible for the Wigner nearest-neighbor level spacing statistics observed in such systems.

ACKNOWLEDGMENTS

B. R. wishes to thank Professor Robert E. Wyatt for his generous hospitality at the University of Texas, Austin, where part of this work was completed.

*Present address: Department of Chemistry, P.O. Box 3159, Louisiana Tech University, Ruston, LA 71272.

¹For reviews, see (a) D. W. Noid, M. L. Koszykowski, and R. A. Marcus, *Annu. Rev. Phys. Chem.* **32**, 267 (1981); (b) B. Eckhardt, *Phys. Rep.* **163**, 205 (1988).

²R. C. Brown and R. E. Wyatt, *Phys. Rev. Lett.* **57**, 1 (1986); *J. Phys. Chem.* **90**, 3590 (1986).

³(a) T. Geisel, G. Radons, and J. Rubner, *Phys. Rev. Lett.* **57**, 2883 (1986); (b) G. Radons, T. Geisel, and J. Rubner, *Adv. Chem. Phys.* **73**, 891 (1989).

⁴S. Fishman, D. R. Grempel, and R. E. Prange, *Phys. Rev. A* **36**, 289 (1987).

⁵L. L. Gibson, G. C. Schatz, M. A. Ratner, and M. J. Davis, *J. Chem. Phys.* **86**, 3263 (1987).

⁶K. G. Kay and B. Ramachandran, *J. Chem. Phys.* **88**, 5688 (1988).

⁷K. G. Kay, *Phys. Scr.* **40**, 360 (1989).

⁸M. J. Davis, *J. Phys. Chem.* **92**, 3124 (1988).

⁹I. C. Percival, *Adv. Chem. Phys.* **36**, 1 (1979).

¹⁰R. T. Swimm and J. B. Delos, *J. Chem. Phys.* **71**, 1706 (1979).

¹¹C. Jaffe and W. P. Reinhardt, *J. Chem. Phys.* **71**, 1862 (1979).

¹²R. Ramaswamy, P. Siders, and R. A. Marcus, *J. Chem. Phys.* **73**, 5400 (1980).

¹³C. Jaffe and W. P. Reinhardt, *J. Chem. Phys.* **77**, 5191 (1982).

¹⁴R. B. Shirts and W. P. Reinhardt, *J. Chem. Phys.* **77**, 5204 (1982).

¹⁵N. De Leon and E. J. Heller, *J. Chem. Phys.* **78**, 4005 (1983); **81**, 5957 (1984); J. Ozment, D. T. Chuljian, and J. Simons, *ibid.* **82**, 4199 (1984).

¹⁶T. Uzer and R. A. Marcus, *J. Chem. Phys.* **81**, 5103 (1984).

¹⁷R. Ramaswamy, *J. Chem. Phys.* **82**, 747 (1985).

¹⁸J. R. Klauder, *Phys. Rev. Lett.* **59**, 748 (1987).

¹⁹M. C. Gutzwiller, *Physica (Amsterdam)* **5D**, 183 (1982).

²⁰C. C. Martens and G. S. Ezra, *J. Chem. Phys.* **83**, 2990 (1985); **86**, 279 (1987).

²¹L. E. Fried and G. S. Ezra, *J. Chem. Phys.* **86**, 6270 (1987).

- ²²E. A. Solov'ev, Zh. Eksp. Teor. Fiz. **75**, 1261 (1978) [Sov. Phys.—JETP **48**, 635 (1978)].
- ²³R. T. Skodje, F. Borondo, and W. P. Reinhardt, J. Chem. Phys. **82**, 4611 (1985).
- ²⁴B. R. Johnson, J. Chem. Phys. **83**, 1204 (1985).
- ²⁵C. W. Patterson, J. Chem. Phys. **83**, 4618 (1985).
- ²⁶T. P. Grozdanov, S. Saini, and H. S. Taylor, Phys. Rev. A **33**, 55 (1986).
- ²⁷T. P. Grozdanov, S. Saini, and H. S. Taylor, J. Chem. Phys. **84**, 3243 (1986).
- ²⁸For reviews of the adiabatic switching method; see (a) R. T. Skodje and J. R. Cary, Comput. Phys. Rep. **8**, 221 (1988); (b) W. P. Reinhardt, Adv. Chem. Phys. **73**, 925 (1989).
- ²⁹C. Jaffe, J. Chem. Phys. **85**, 2885 (1986); C. Jaffe and M. Watanabe, *ibid.* **89**, 6329 (1988); C. Jaffe, *ibid.* **86**, 4499 (1987).
- ³⁰S.-W. Cho and K. G. Kay, J. Phys. Chem. **92**, 602 (1988).
- ³¹R. S. MacKay, J. D. Meiss, and I. C. Percival, Physica (Amsterdam) **13D**, 55 (1984).
- ³²D. Bensimon and L. P. Kadanoff, Physics (Amsterdam) **13D**, 82 (1984).
- ³³M. J. Davis, Chem. Phys. Lett. **110**, 491 (1984); J. Chem. Phys. **83**, 1016 (1985).
- ³⁴M. J. Davis and S. K. Gray, J. Chem. Phys. **84**, 5389 (1986).
- ³⁵S. K. Gray, S. A. Rice, and M. J. Davis, J. Phys. Chem. **90**, 3470 (1986).
- ³⁶M. J. Davis, J. Chem. Phys. **86**, 3978 (1987).
- ³⁷R. T. Skodje and M. J. Davis, J. Chem. Phys. **88**, 2429 (1988).
- ³⁸I. C. Percival and D. Richards, Adv. At. Mol. Phys. **11**, 2 (1975).
- ³⁹A. P. Clark, A. S. Dickenson, and D. Richards, Adv. Chem. Phys. **36**, 63 (1977).
- ⁴⁰C. Jaffe and P. Brumer, J. Chem. Phys. **82**, 2330 (1985).
- ⁴¹M. Hénon and C. Heiles, Astron. J. **69**, 73 (1964).
- ⁴²D. W. Noid and R. A. Marcus, J. Chem. Phys. **67**, 559 (1977).
- ⁴³R. T. Skodje and F. Borondo, Chem. Phys. Lett. **118**, 409 (1985).
- ⁴⁴B. Ramachandran and K. G. Kay, J. Chem. Phys. **86**, 4628 (1987).
- ⁴⁵M. J. Davis and E. J. Heller, J. Chem. Phys. **75**, 246 (1981).
- ⁴⁶G. B. Powell and I. C. Percival, J. Phys. A **12**, 2053 (1979).
- ⁴⁷R. A. Marcus, in *Horizons in Quantum Chemistry, Proceedings of the Third International Congress in Quantum Chemistry, Kyoto, 1979*, edited by K. Fukui and B. Pullman (Reidel, Dordrecht, 1980), p. 107.
- ⁴⁸D. W. Noid, M. L. Koszykowski, M. Tabor and R. A. Marcus, J. Chem. Phys. **72**, 6168 (1980); D. W. Noid, M. L. Koszykowski, and R. A. Marcus, Chem. Phys. Lett. **73**, 269 (1980).
- ⁴⁹R. Ramaswamy and R. A. Marcus, J. Chem. Phys. **74**, 1379 (1981); **74**, 1385 (1981).
- ⁵⁰R. A. Marcus, Faraday Discuss. Chem. Soc. **75**, 103 (1983).
- ⁵¹A. M. Ozorio de Almeida, J. Phys. Chem. **88**, 6139 (1984).
- ⁵²M. V. Berry, in *Chaotic Behavior in Quantum Systems*, edited by G. Casati (Plenum, New York, 1985).
- ⁵³K. G. Kay, J. Chem. Phys. **72**, 5955 (1980).
- ⁵⁴S. N. Rai and K. G. Kay, J. Chem. Phys. **80**, 4961 (1984).
- ⁵⁵M. J. Davis and E. J. Heller, J. Chem. Phys. **80**, 5036 (1984).
- ⁵⁶G. Hose, H. S. Taylor, and Y. Y. Bai, J. Chem. Phys. **80**, 4363 (1984); K. Stefanski and H. S. Taylor, Phys. Rev. A **31**, 2810 (1985).
- ⁵⁷B. K. Holmer and M. S. Child, Faraday Discuss. Chem. Soc. **75**, 131 (1983).
- ⁵⁸Y. Y. Bai, G. Hose, K. Stefanski, and H. S. Taylor, Phys. Rev. A **31**, 2821 (1985).
- ⁵⁹K. M. Christofel and P. Brumer, Phys. Rev. A **33**, 1309 (1986).
- ⁶⁰See, for example, C. Cohen-Tannoudji, B. Diu, and F. Laloë, *Quantum Mechanics* (Wiley, New York, 1977), Vol. 1, Chap. 4, p. 408.
- ⁶¹D. W. Noid, M. L. Koszykowski, and R. A. Marcus, J. Chem. Phys. **78**, 4018 (1983).
- ⁶²T. Uzer, D. W. Noid, and R. A. Marcus, J. Chem. Phys. **79**, 4412 (1983).
- ⁶³D. Farrelly and W. P. Reinhardt, J. Chem. Phys. **78**, 606 (1983).
- ⁶⁴W. P. Reinhardt, in *Chaotic Behavior in Quantum Systems*, edited by G. Casati (Plenum, New York, 1985).
- ⁶⁵E. J. Heller, Faraday Discuss. Chem. Soc. **75**, 141 (1983).
- ⁶⁶M. Wilkinson, J. Phys. A **20**, 635 (1987).
- ⁶⁷R. T. Lawton and M. S. Child, Mol. Phys. **44**, 709 (1981).
- ⁶⁸M. V. Berry, J. Phys. A **17**, 1225 (1984).
- ⁶⁹E. L. Sibert, J. T. Hynes, and W. P. Reinhardt, J. Chem. Phys. **77**, 3595 (1982).
- ⁷⁰M. V. Berry, Ann. Phys. **131**, 163 (1981).
- ⁷¹M. Robnik, J. Phys. A **17**, 1049 (1984).
- ⁷²A. Peres, in *Chaotic Behavior in Quantum Systems*, edited by G. Casati (Plenum, New York, 1985).
- ⁷³O. Bohigas, M. J. Gionnoni, and C. Schmidt, in *Quantum Chaos and Statistical Nuclear Physics*, Vol. 263 of *Lecture Notes in Physics* (Springer, Berlin, 1986); see especially Figs. 13 and 14.
- ⁷⁴For an opposing view, see Refs. 64 and 65.
- ⁷⁵A collection of fundamental papers can be found in C. E. Porter, *Statistical Theories of Spectra: Fluctuations* (Academic, New York, 1965).
- ⁷⁶For recent reviews, see Ref. 1(b) and Th. Zimmerman, L. S. Cederbaum, H.-D. Meyer, and H. Koppel, J. Phys. Chem. **91**, 4446 (1987).
- ⁷⁷B. Eckhardt, G. Hose, and E. Pollak, Phys. Rev. A **39**, 3776 (1989).
- ⁷⁸B. V. Chirikov, Phys. Rep. **52**, 265 (1979); G. M. Zaslavski and B. V. Chirikov, Usp. Fiz. Nauk **105**, 3 (1972) [Sov. Phys.—Usp. **14**, 549 (1972)].
- ⁷⁹S. Graffi, T. Paul, and H. J. Silverstone, Phys. Rev. Lett. **59**, 255 (1987); Phys. Rev. A **37**, 2214 (1988).
- ⁸⁰W. H. Miller, J. Chem. Phys. **48**, 1651 (1968).